The progress of beam-beam simulation and related researches of STCF

Sangya Li

University of Science and Technology of China

2024/09/02

Super Tau Charm Facility (STCF)

Haiping Peng , FTCF, USTC, 2024

STCF: A natural and feasible extension project of BEPCII/ BESIII in the near future, China's preferred medium-term strategy in particle physics

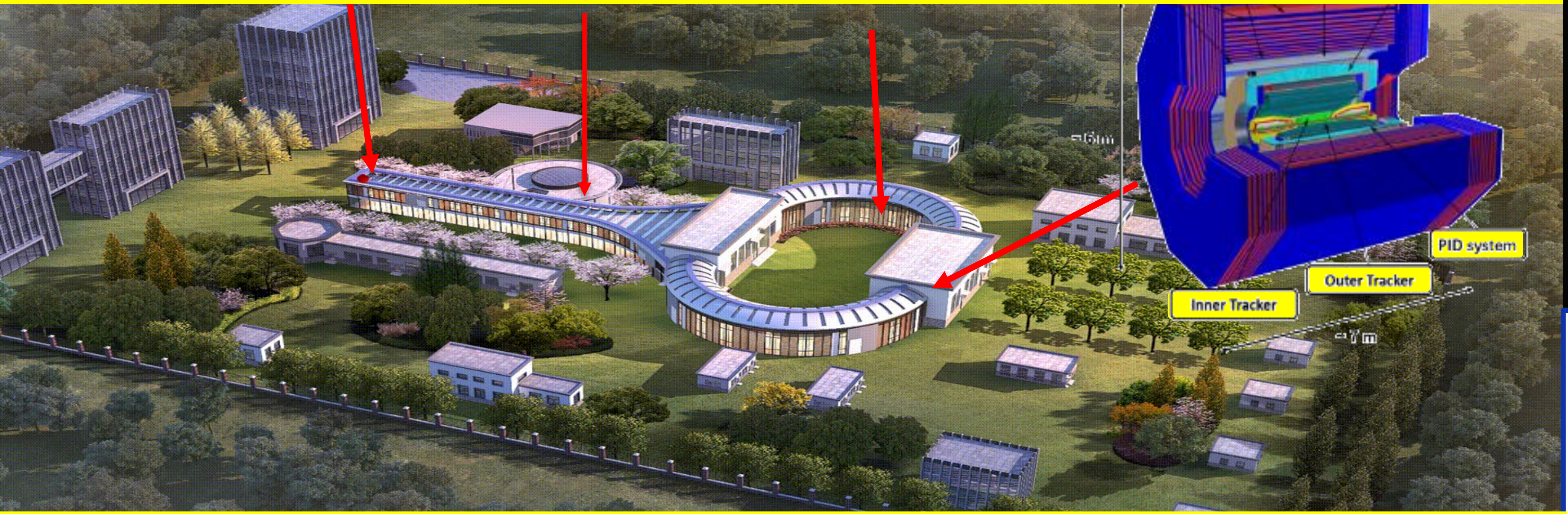

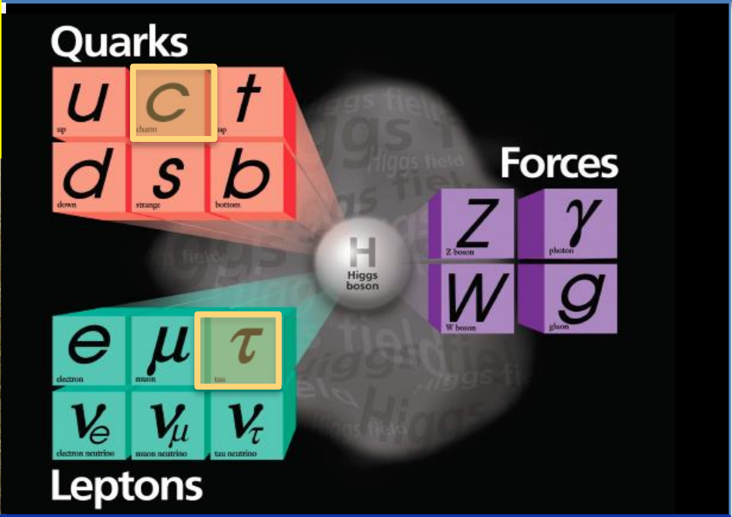

Deliver a massive amount of taus and hadrons composed of charm quark, allow for the studies of particle composition, the deep structure of matter, as well as the fundamental interaction forces

- E_{cm}= 2-7 GeV, $\mathcal{L} > 0.5\times10^{35}$ cm $^{-2}$ s $^{-1}$
- Potential for upgrade to increase luminosity and realize polarized beam
- Site: 1 km^2, Hefei's suburban "Future Big Science City"

- 14th five-years plan (2021-2025): Conceptual design and R&D of Key technology, 5 years, 0.42 B CNY
- 15th five-years plan (2026-2030): Construction 6 years, 4.5 B CNY
- Operating for 10 years, upgrade for 3 years, operating again for another 8 years

Introduction to the research work on beam-beam interaction

Research emphasis of Beam-Beam Interaction:

- Achieving Stable High Luminosity through Optimization of Beam-Beam Parameters to Guide Lattice Design:

  - Selection of working points to avoid harmful resonance lines.
  - Choice of μ_s and crossing angle to achieve more stable high-luminosity regions.
  - Limits on current → bunch particle number → beam-beam parameters.

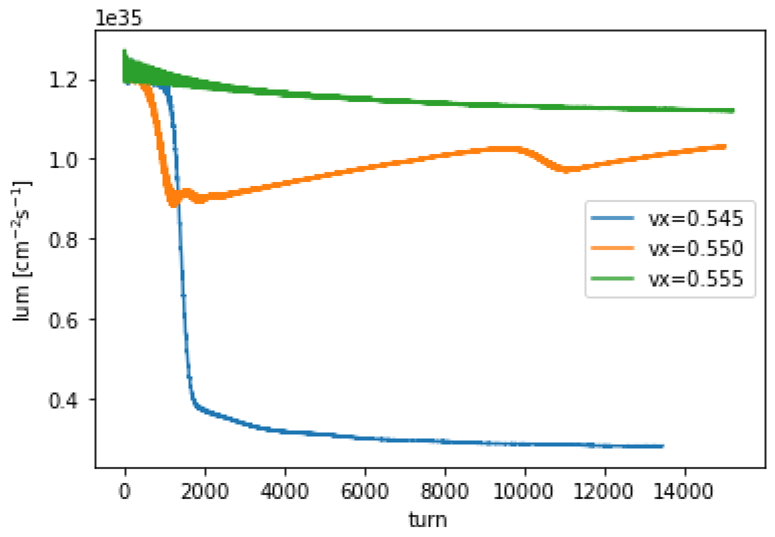

Luminosity simulation results for different working points in the 800m lattice.

Research emphasis of Beam-Beam Interaction:

- Exploring the Impact of Beam-Beam Interaction and Beam Instability under Extreme Luminosity Conditions:
  - One of our key research areas is investigating new instabilities caused by the increase in the beam-beam parameter ξy when using the crab waist scheme under large Piwinski angles. Due to the coupling between the longitudinal and transverse planes, the beam-beam interaction is essentially three-dimensional. We will focus on effects such as coherent X-Z instability and 3D triggers to fully understand their impact on collider performance.
  - Another focus is the coupling between beam-beam interaction and lattice nonlinearity and impedance. This includes considering the vertical beam-beam interaction and ring impedance, as well as strong coherent positive tail instability related to the transverse mode coupling instability threshold. Special attention will be given to the relationship between nonlinear factors introduced by the crab sextupole and beam-beam interaction.

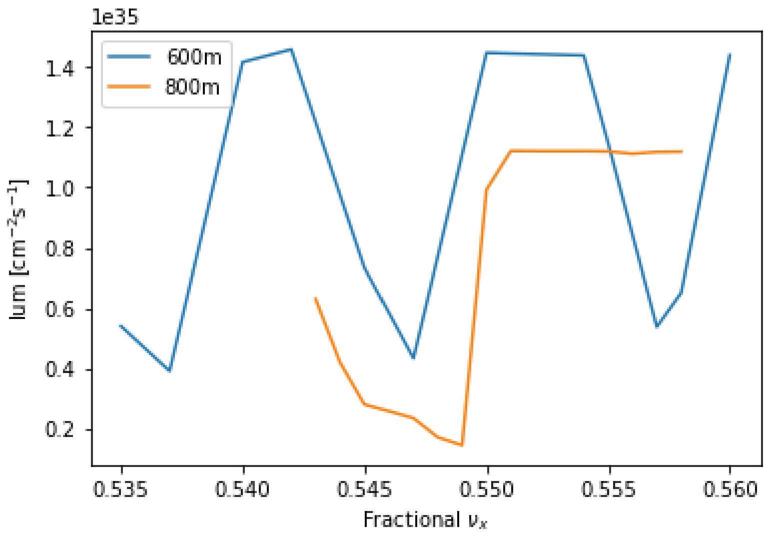

The impact of X-Z instability is relatively small in the 800m lattice.

Beam-beam simulation code

- **Weak-strong model**: Multi-macro particle model and single-macro particle model.
  - ➢ Strong Beam: Fixed Gaussian distribution, unaffected by the weak beam.
  - ➢ Weak Beam: The transverse field effect of the strong beam is calculated using the Bassetti-Erskine formula; the crossing angle is handled by introducing a Lorentz transformation; the finite bunch length allows for longitudinal slicing of the strong beam.
  - ➢ Advantages: Low computational cost (equivalent to introducing only one additional nonlinear element).
  - ➢ Disadvantages: Not self-consistent, unable to simulate complex instabilities such as coupling impedance.
  - ➢ Current Usage: BBWS.
- **Strong-Strong Model:** Both bunches are fully modeled using macroparticles.
  - ➢ The beam-beam interaction is calculated using the Particle-In-Cell (PIC) method, or by first fitting a Gaussian distribution and then applying the Bassetti-Erskine formula.
  - ➢ Compared to the weak-strong model, it includes:
    (1) Beam-beam interaction at the IP can account for beamstrahlung.
    (2) The linear mapping during arc transport includes synchrotron radiation effects (damping + fluctuation).
    (3) The influence of the full-ring longitudinal wakefield is included at the IP before the collision.
  - ➢ Disadvantages: High computational cost.
    Advantages: Self-consistent and more accurate.
  - ➢ Current Usage: IBB, BBSS.
    • Particle In Cell (PIC)
    • Gaussian approximation.
- **Lattice transformation** compatible with SAD (by Li Zhiyuan, APES-T).
  - ➢ • Developed by cuda (nvcc) on NVIDIA GPU

IBB, Y.Zhang , IHEP
BBWS, BBSS K. Ohmi ,KEK

2

Simulation of beam- beam interaction at 600m

600m lattice

❑ The important changes

- Circumference 702 → 616.76 m
- β_x^* 90 → 40 mm
- ε_y 20.8 → 22.35 pm
- Momentum compaction factor
- Energy spread

} Natural bunch length

ξ_y 0.0855 → 0.111

Parameters	Units	STCF
Optimal beam energy, E	GeV	2
Circumference, C	m	616.76
Crossing angle, 2θ	mrad	60
Relative gamma		3913.9
Revolution period, T_0	μs	2.057
Revolution frequency, f_0	kHz	486.08
Horizontal emittance, ε_x	nm	4.47
Coupling, k		0.50%
Vertical emittance, ε_y	pm	22.35
Hor. beta function at IP, β_x	mm	40
Ver. beta function at IP, β_y	mm	0.6
Hor. beam size at IP, σ_x	μm	13.37
Ver. beam size at IP, σ_y	μm	0.116
Betatron tune, ν_x/ν_y		31.552/24.572
Momentum compaction factor, α_p	10^{-4}	10.27
Energy spread, σ_ε	10^{-4}	8.77
Beam current, I	A	2
Number of bunches, n_b		512
Single-bunch current, I_b	mA	3.91
Particles per bunch, N_b	10^{10}	5.02
Single-bunch charge	nC	8.04
Energy loss per turn, U_0	keV	273
Hor. damping time, τ_x	ms	30.14
Ver. damping time, τ_y	ms	30.14
Long. damping time, τ_z	ms	15.07
RF frequency, f_{RF}	MHz	497.5
Harmonic number, h		1024
RF voltage, V_{RF}	MV	1.2
Synchronous phase, ϕ_s	deg	167
Synchrotron tune, ν_z		0.0099
Bunch length, σ_z	mm	8.94
Natural bunch length, σ_z	mm	8.94
RF bucket height, $(\Delta E/E)_{max}$	%	1.56
Piwinski angle, ϕ_{Piw}	rad	20.06
Hor. beam-beam parameter, ξ_x		0.0032
Ver. beam-beam parameter, ξ_y		0.111
Equivalent bunch length, σ_{z_e}	mm	0.45
Hour-glass factor, F_h		0.9066
Luminosity, L	$cm^{-2}s^{-1}$	1.45E+35

Input parameters   parameters from lattice design
also input parameters   output parameters (use formula)

Verification of luminosity at 600m operating point:

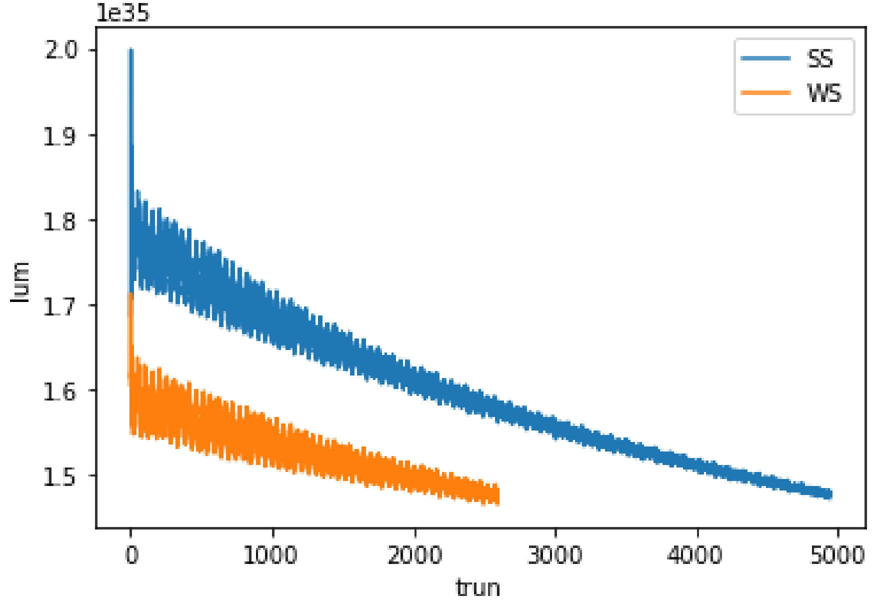

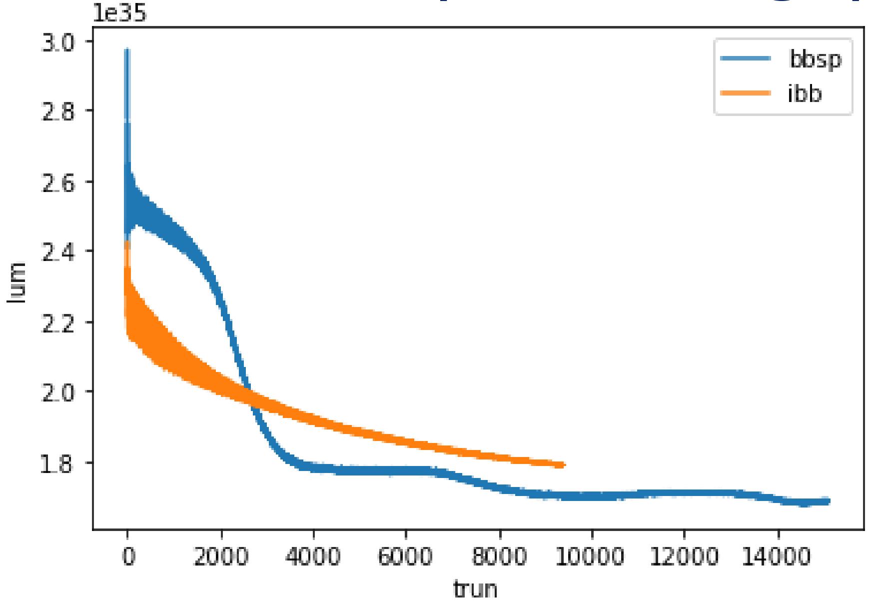

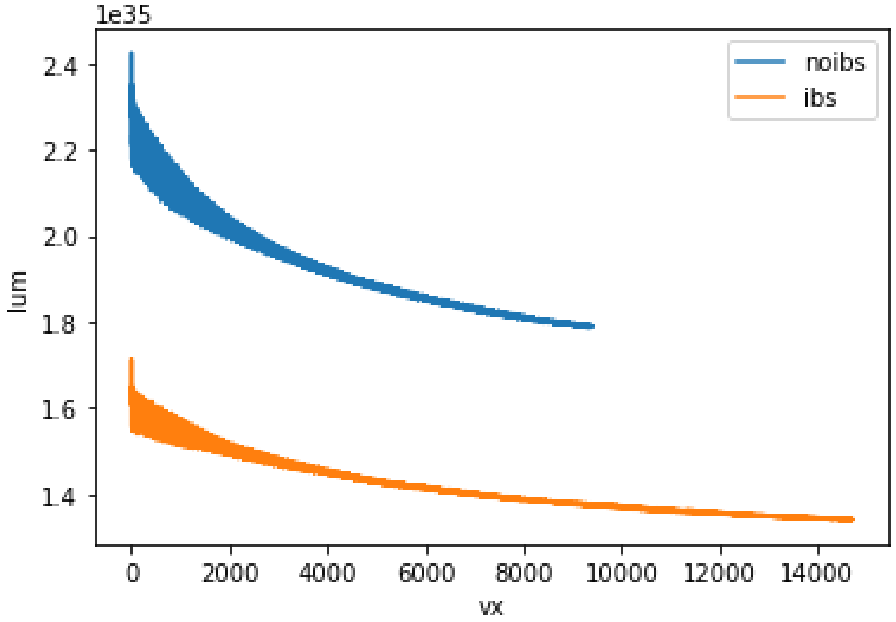

comparison of parameters	STCF (v3)
L (m)	616.76
βy*	0.6mm
peak luminosity	1.4e35 $cm^{-2}\ s^{-1}$
ξx/ξy	0.0038/0.106
νz	0.0096
design bunch population	5.02e10
σx /σy (μm)	15.19/0.132
σz (mm)	8.21(vs natural bunch length8.2)

The influence of current intensity on the luminosity of 600m:

- **change with different number of particles**

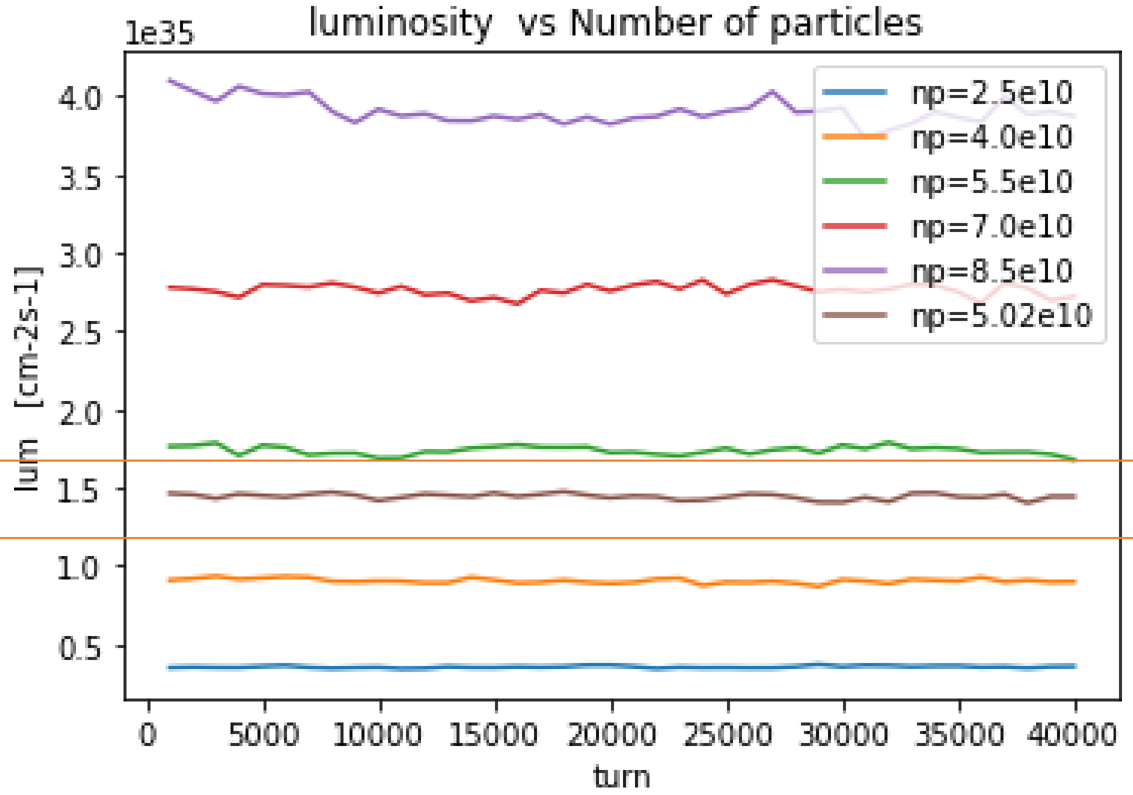

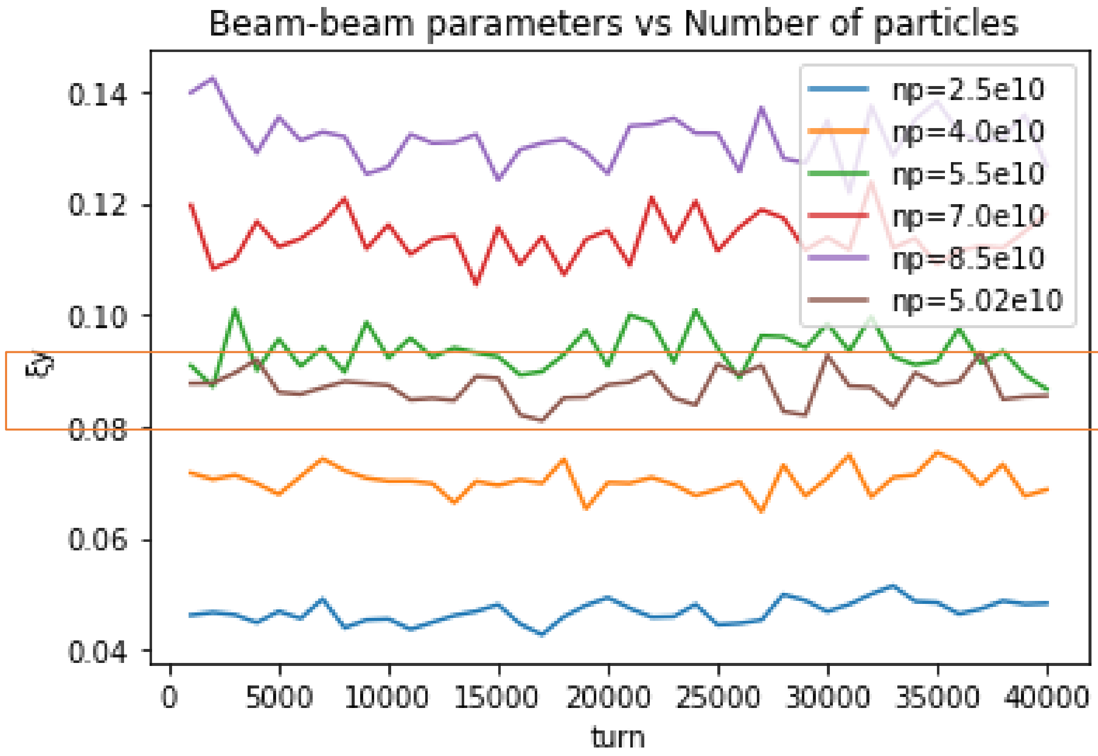

Dependence on convective strength at design operating point (552,572)

The impact of X-Z instability on 600m luminosity:

Beam-beam simulation results from IBB

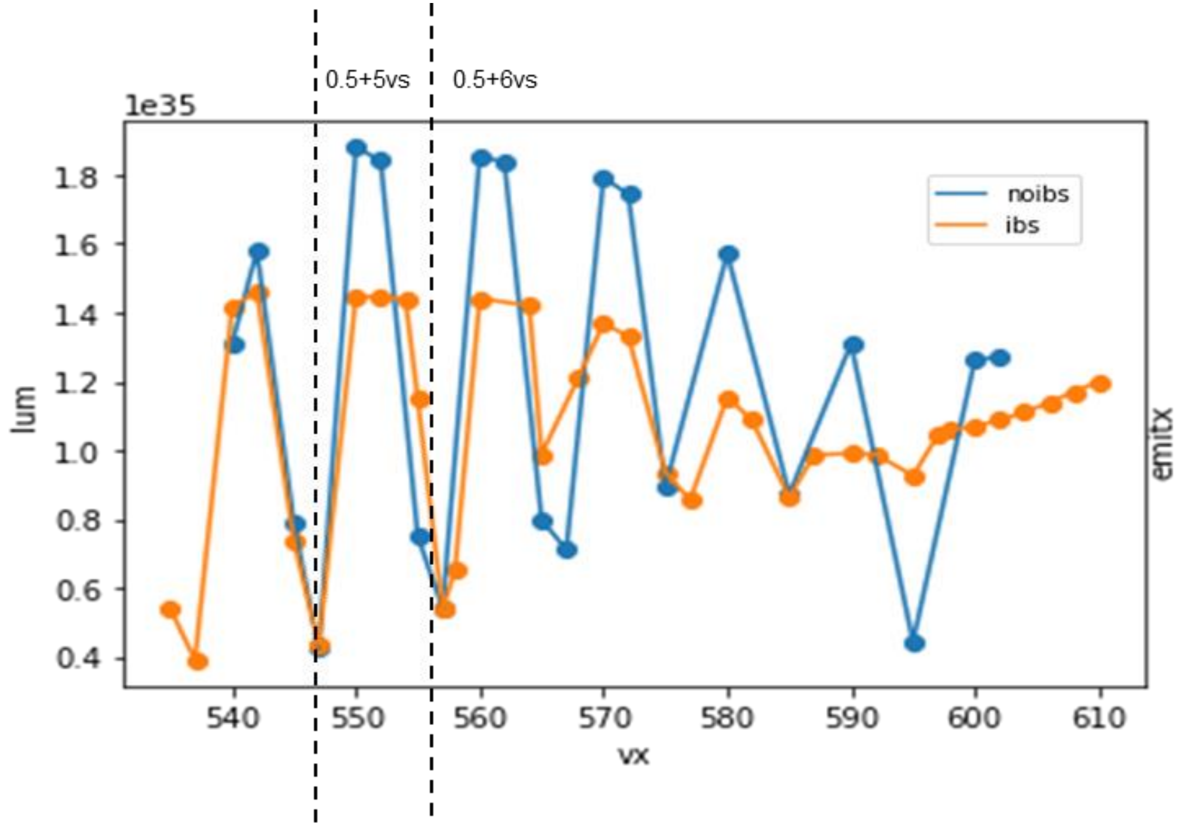

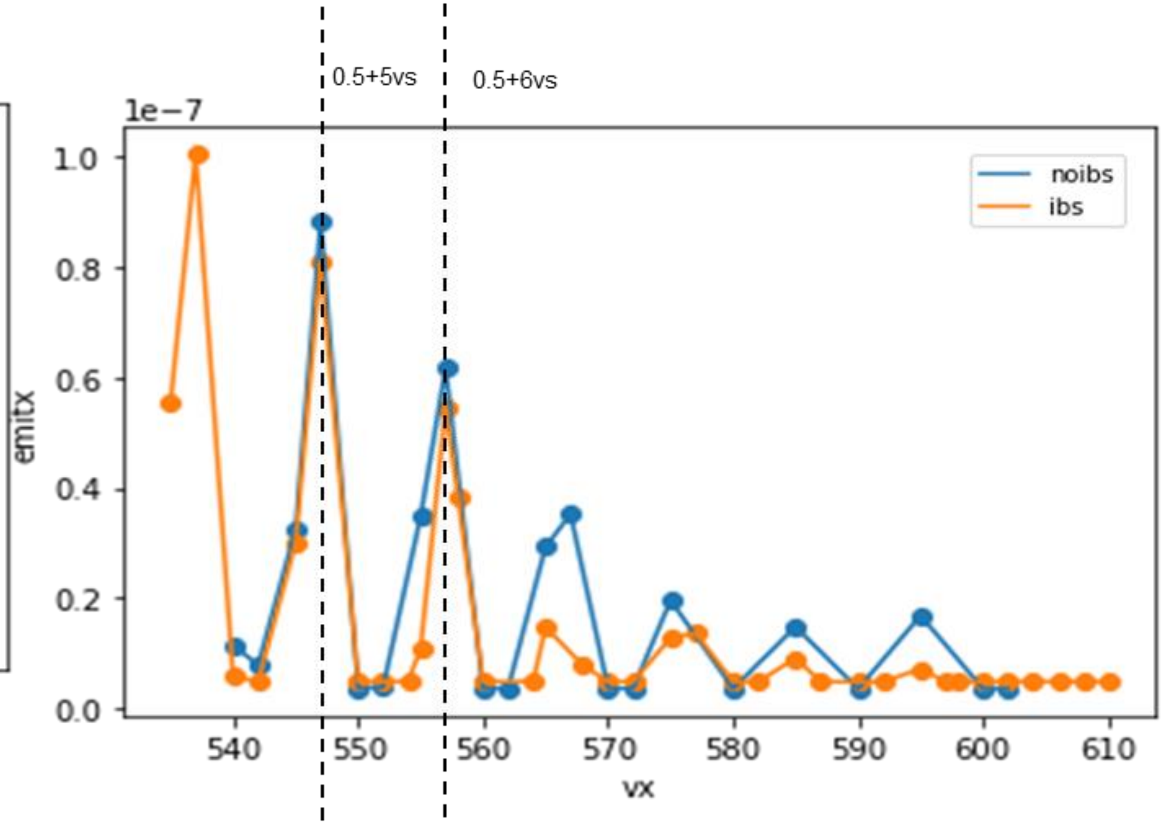

- There is strong X-Z instability near the designed operating point.

SS result

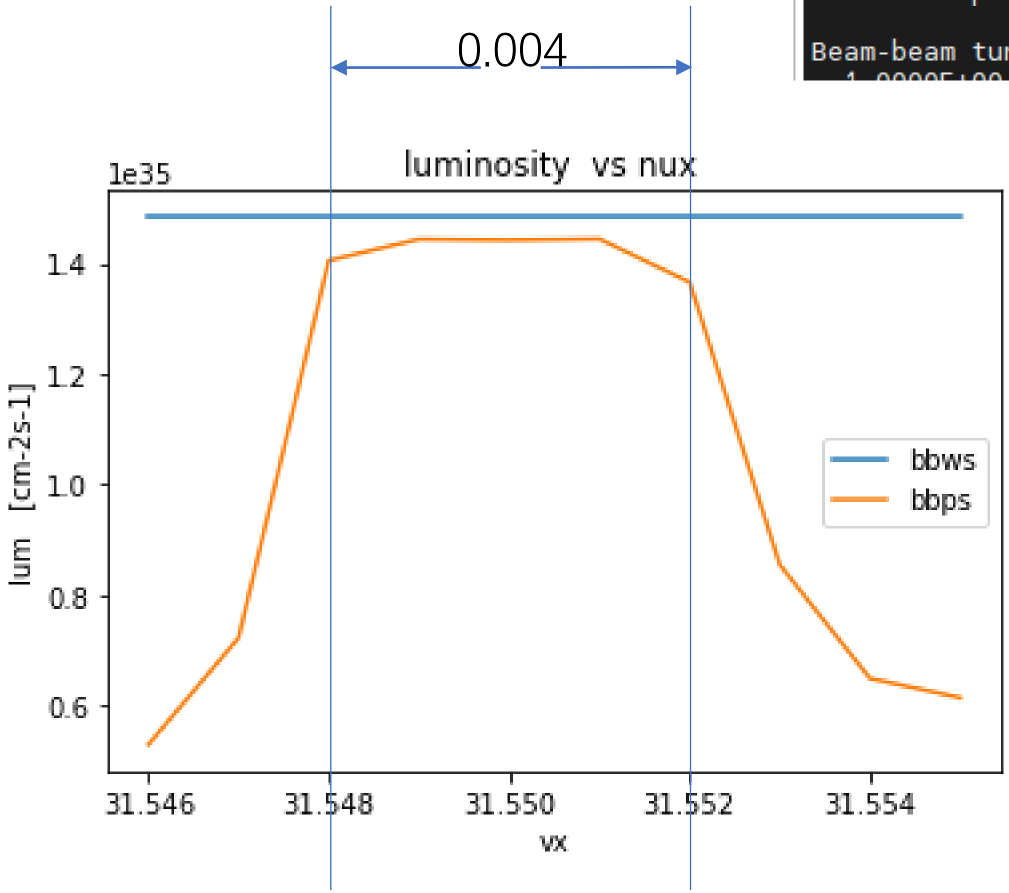

2θ =0.06 nvy = .572

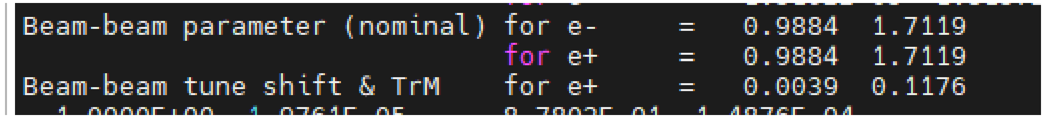

Close to xix

- In the X-Z resonance, the stable high-luminosity region is relatively narrow.
- Adjustment direction:
  - 1. Adjust the μ s ;
  - 2. Turn down θ;
  - 3. Reduce beta βx , σx

The impact of νs on the luminosity of 600m:

☐ Adjustment of nus

- Smaller nus narrow the resonance, more disturbance
- Bigger nus widens the distance between vertical resonances

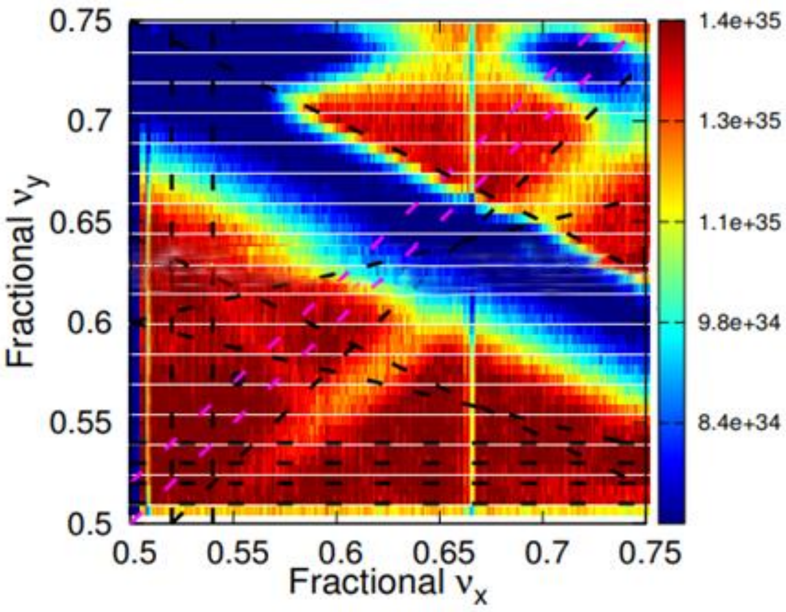

nus =0.005

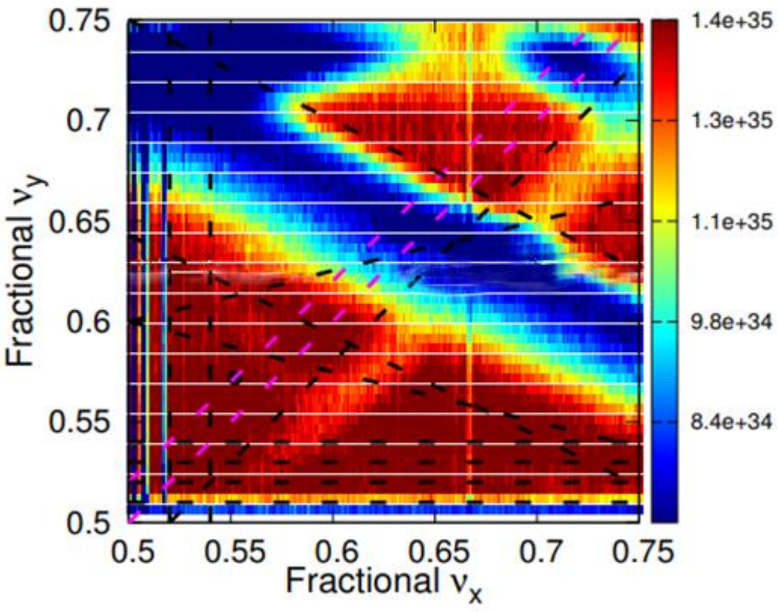

nus=0.0099(design)

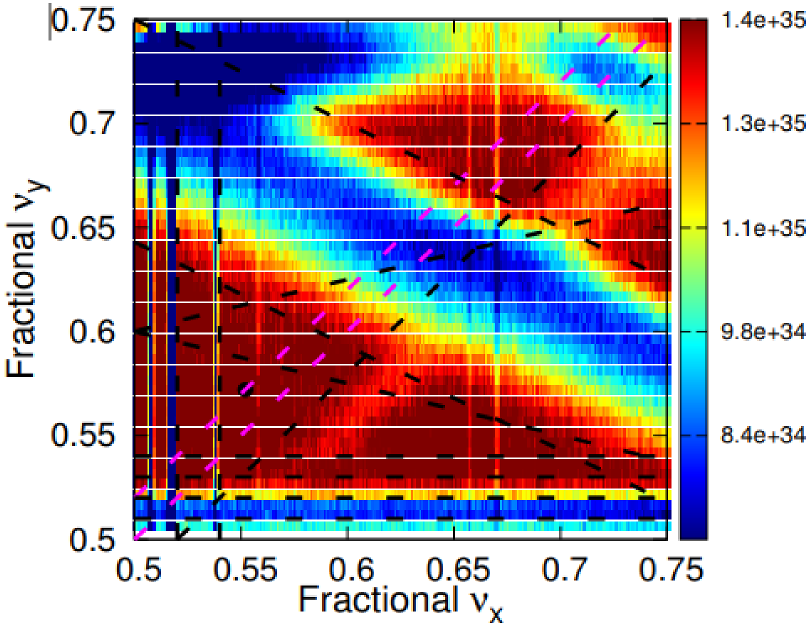

nus =0.02

Beam-beam simulation results from BBWS

The impact of νs on X-Z instability:

Beam-beam simulation results from IBB

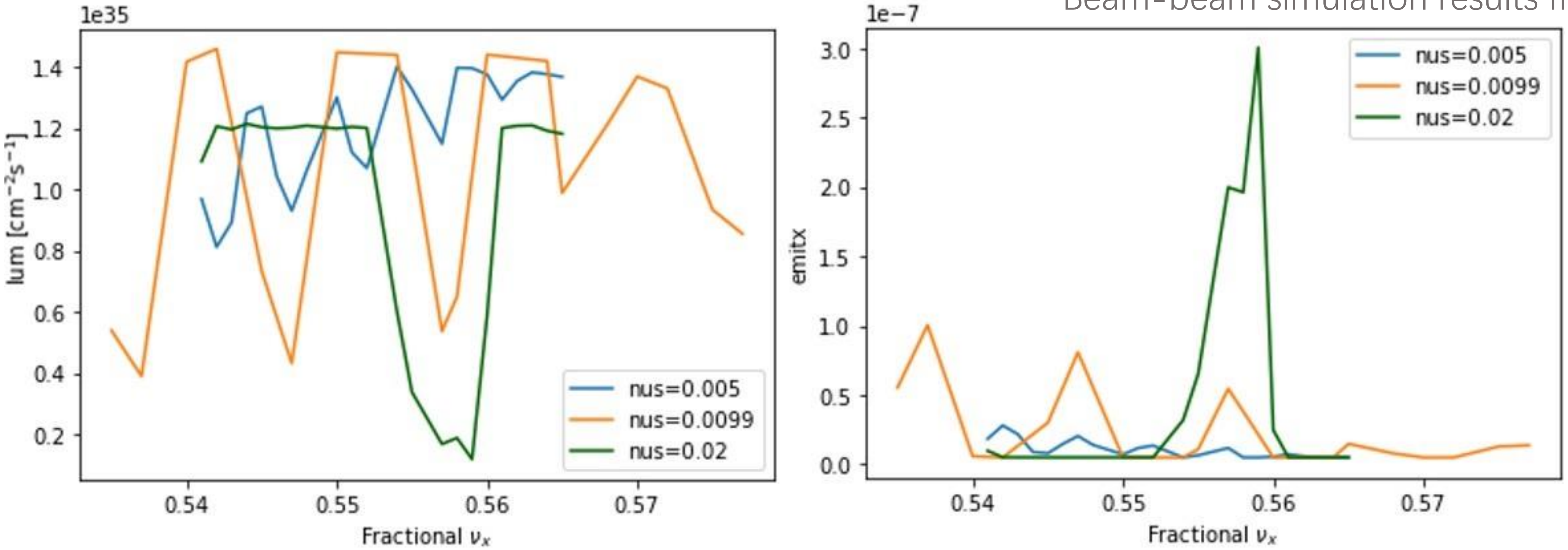

- The X-Z instability can be adjusted by changing νs .
- Increasing νs from 0.0099 to 0.02 significantly broadens the stable high-luminosity region, but slightly decreases the peak luminosity.
- The luminosity degradation caused by X-Z instability weakens as νs decreases, but it becomes more concentrated.

The impact of the crossing angle on 600m luminosity：

$$L_i = \frac{\sigma_z}{\sqrt{1+\phi^2}} \approx \frac{\sigma_x}{\theta}$$

Smaller crossing angle higher luminosity.

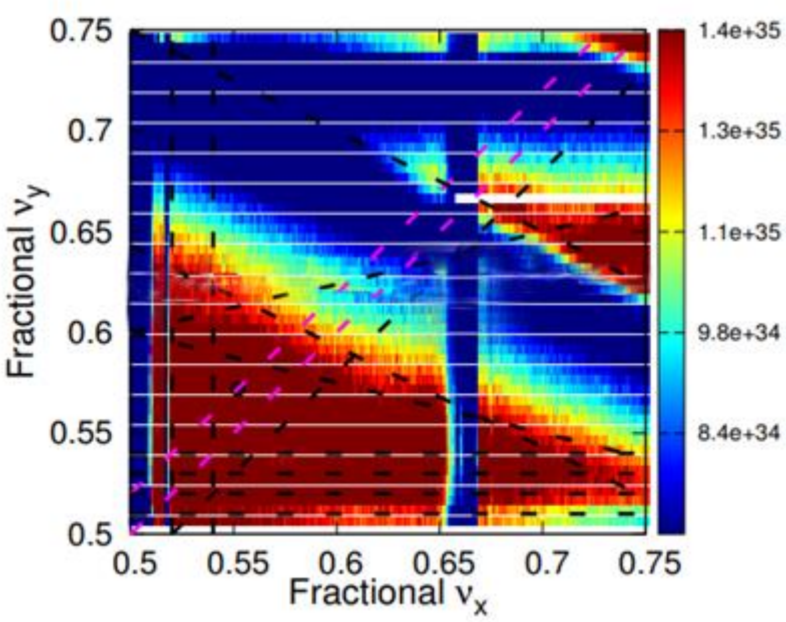

2θ =0.04

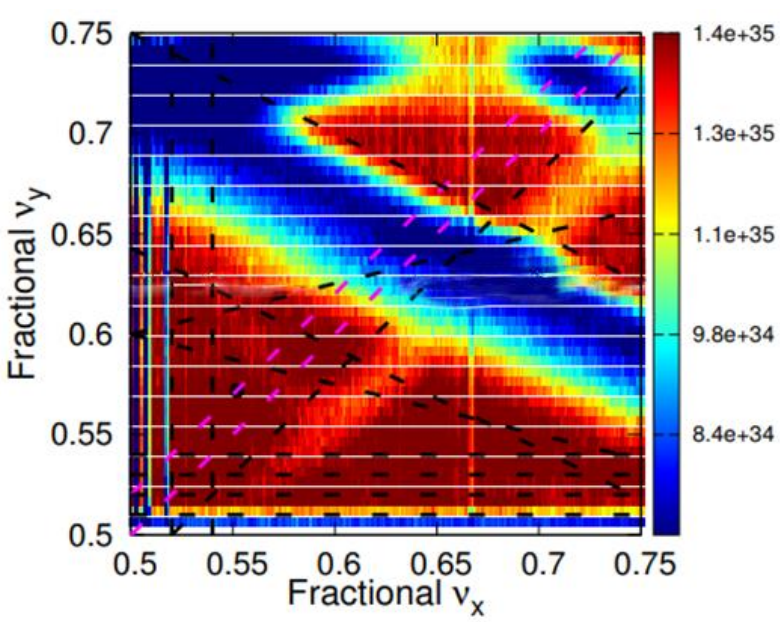

2θ=0.06(design)

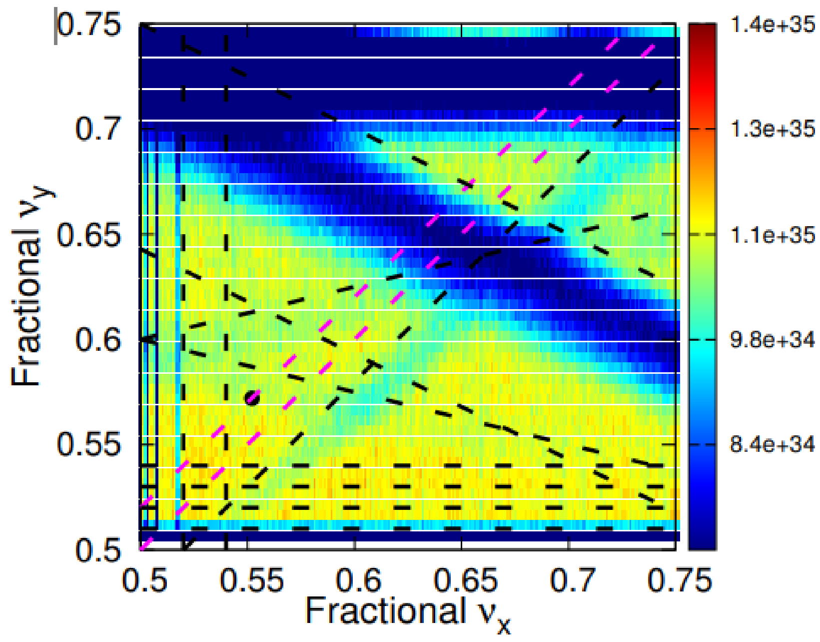

2θ =0.08

- The luminosity does not significantly increase when the crossing angle is decreased.

XZ Instability at Different Crossing Angles:

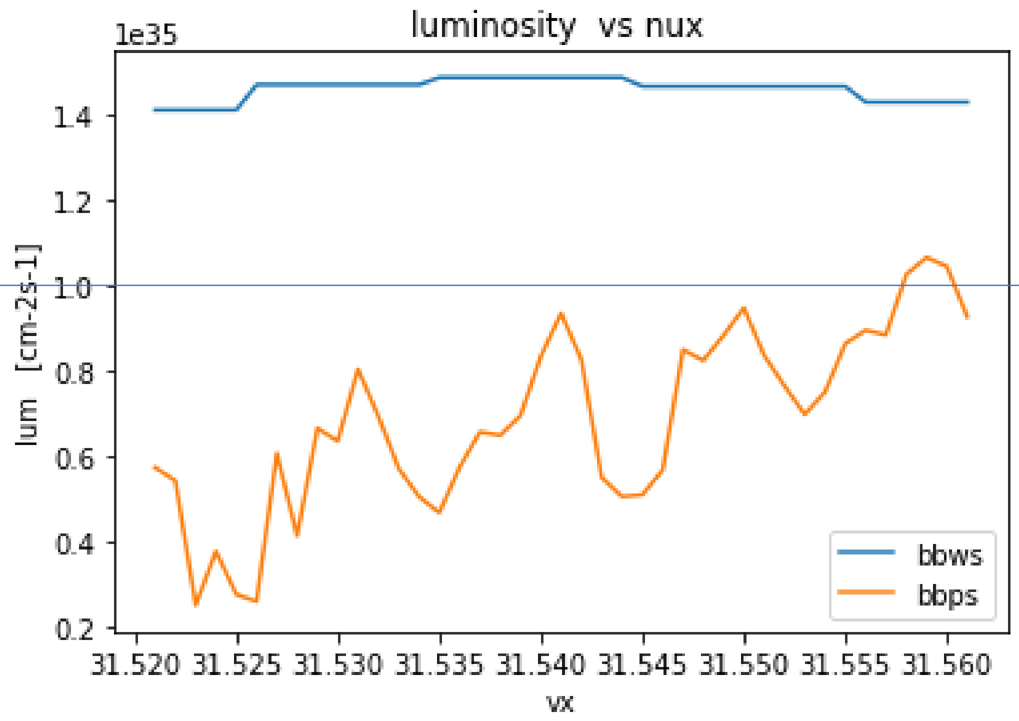

2θ =0.04 nvy = .545

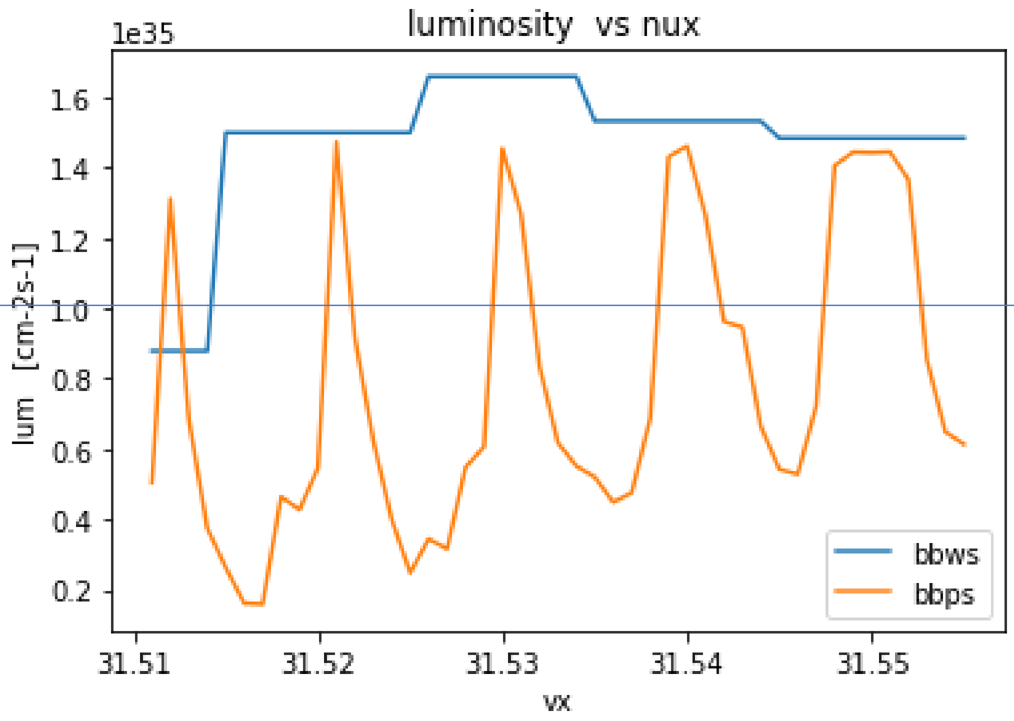

2θ =0.06 nvy = .572

Beam-Beam Simulation Results for 600m with Lattice:

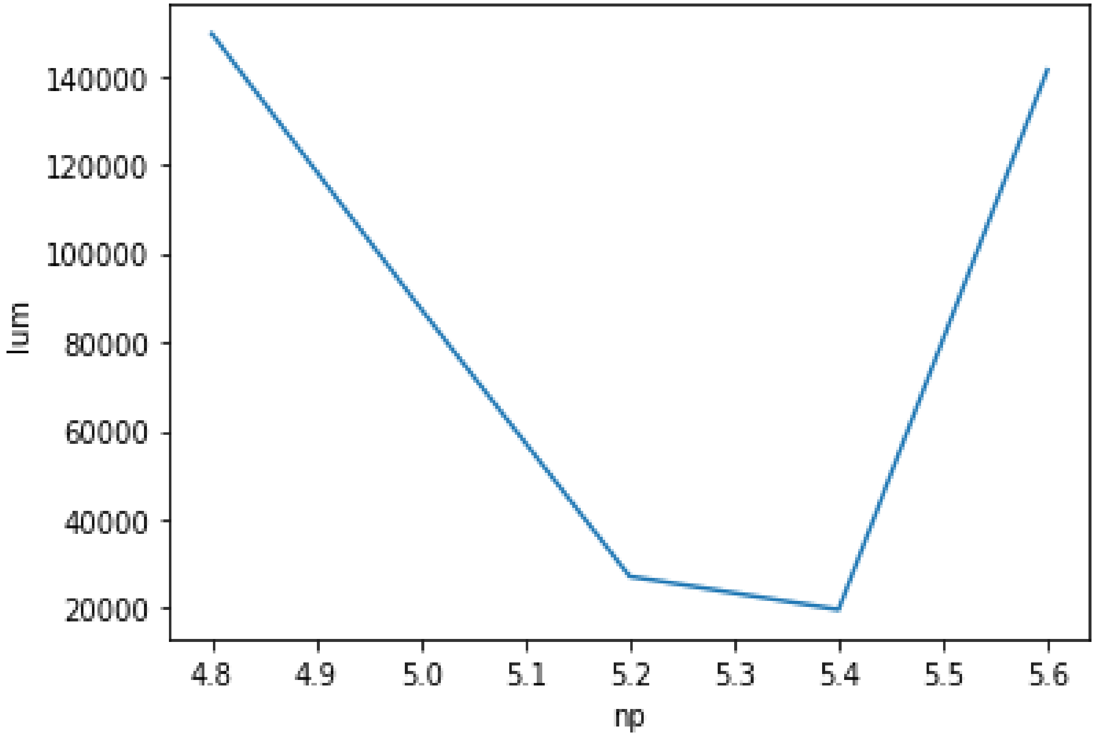

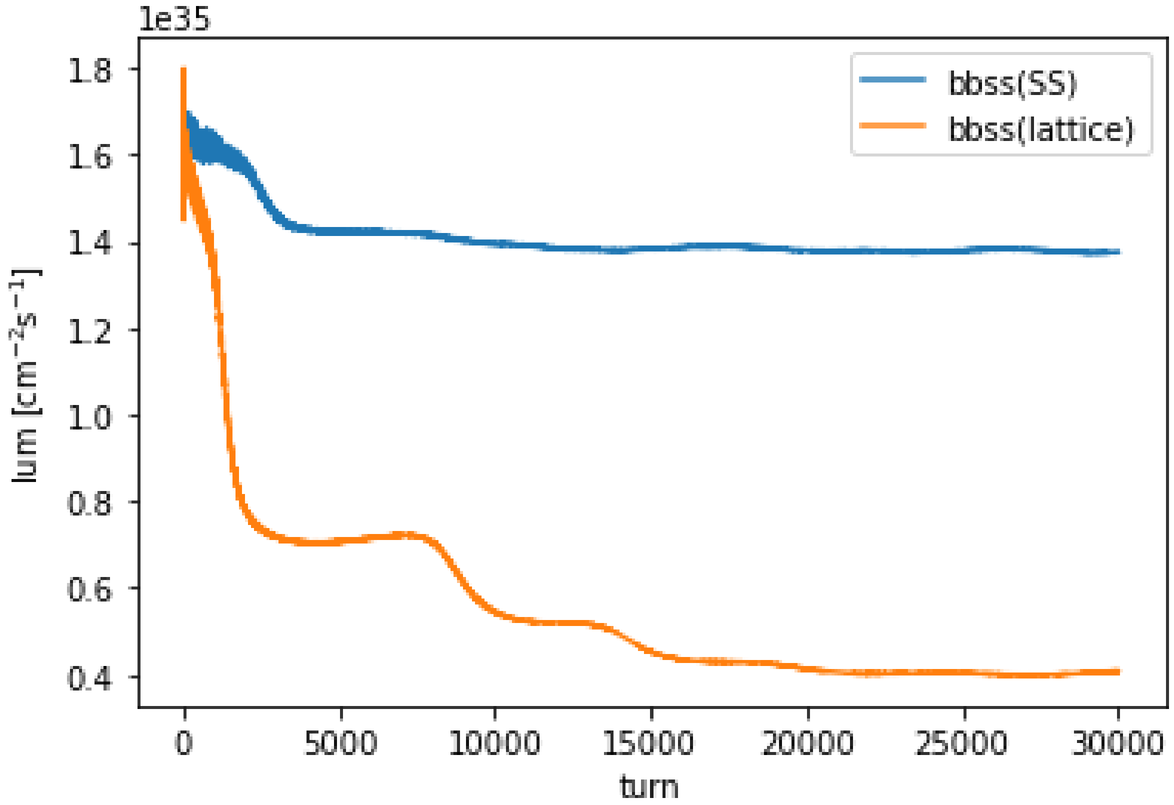

- The instability caused by the lattice further narrows the range of stable working points, making the originally designed working point unstable.
- The luminosity at the designed working point drops significantly, failing to meet the design target.

Challenges on IR design for new-generation e+e- colliders

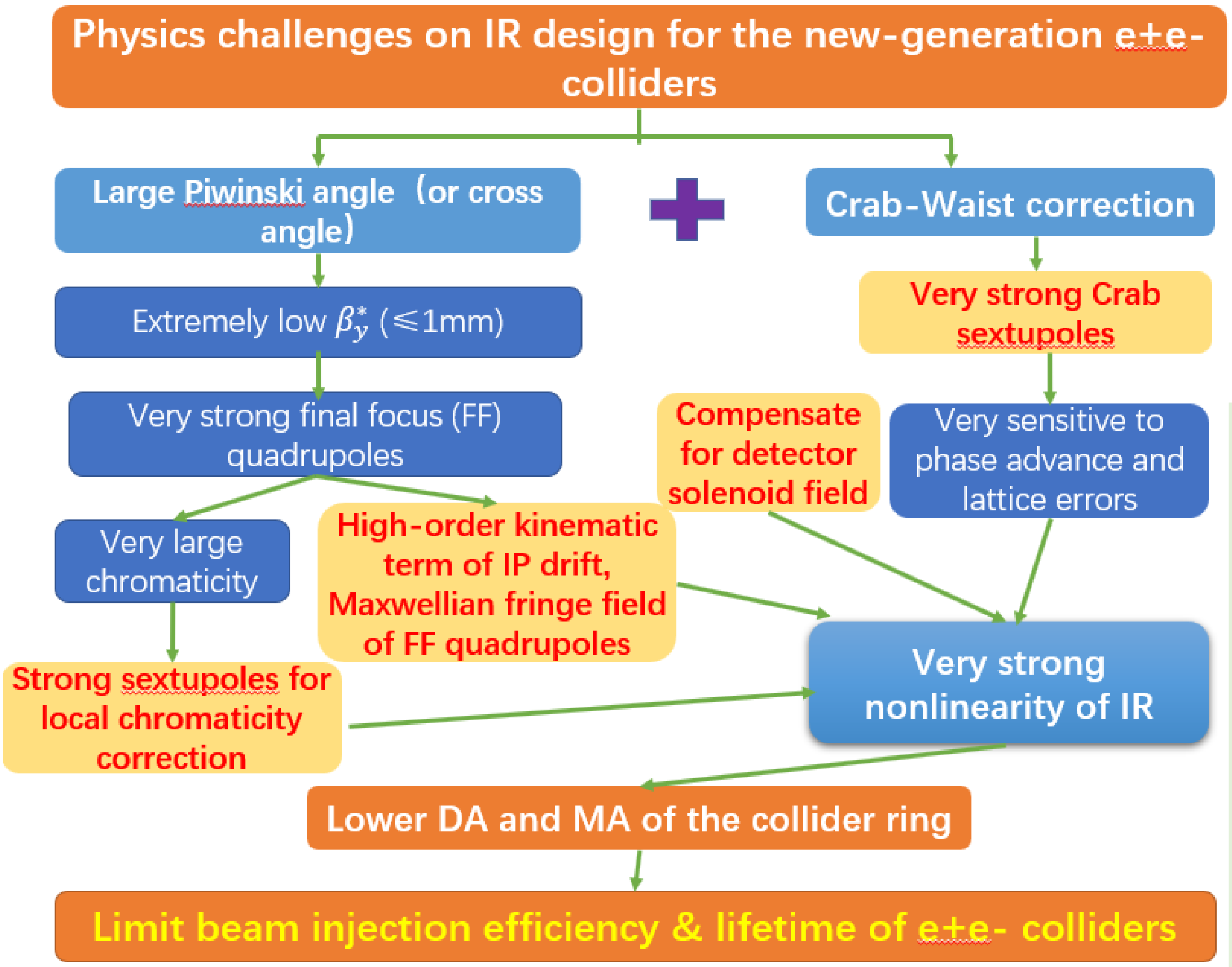

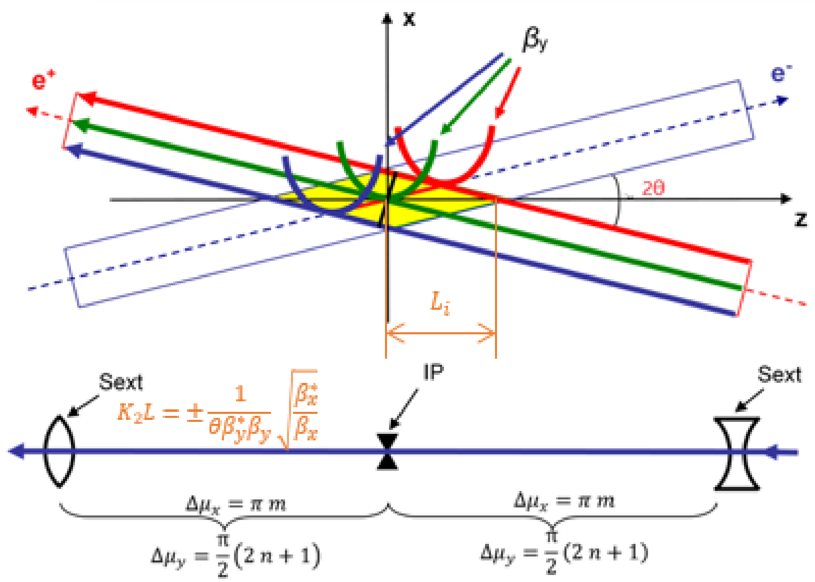

The choice of β_y^* and L^* and crossing angle 2θ for STCF:

- A large crossing angle of 60 mrad can achieve rapid separation of the two beams and avoid parasitic collisions;

→ $L^* \geq 0.9$m is required to provide sufficient space for installation of the dual-aperture quadrupole QD0 .

→ β_y^* of 0.6mm is now set to achieve the goal luminosity of 10^{35} cm^{-2}s^{-1}, (as reducing β_y^* is the most effective way to increase luminosity). However, probably β_y^* can be raised to 0.8mm from 0.6mm, helping mitigate chromaticity and nonlinearity, with same luminosity.

D. Zhou, USTC seminar, 2023
Linhao Zhang USTC, 2024

• Change the chromaticity

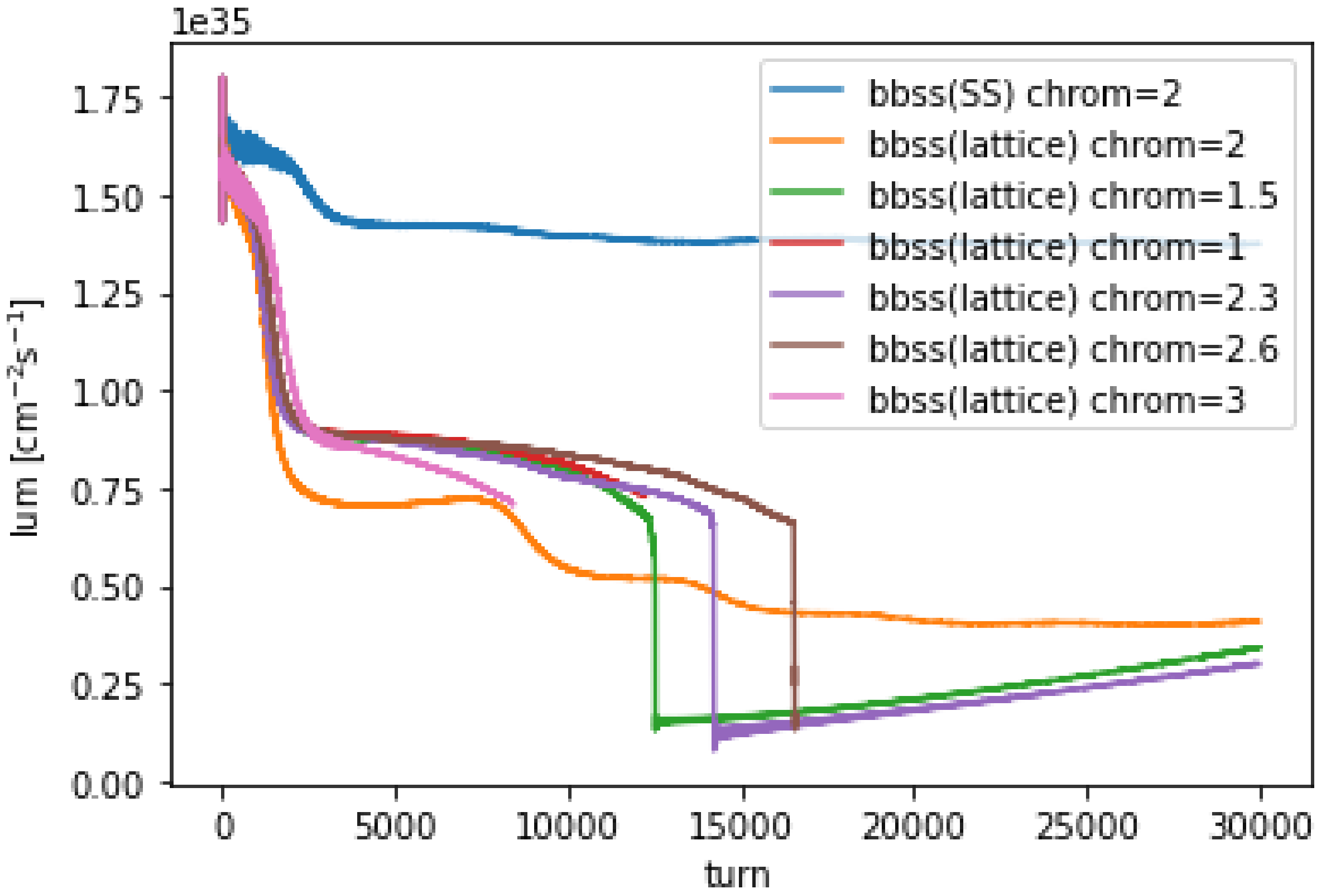

- With the working point unchanged, adjust CCY and CCX sextupoles to control chromaticity.
- The results do not directly indicate whether chromaticity is the cause of beam instability introduced by the lattice.

3

Beam-Beam Interaction Simulation Study for 800m

800m VS 600m:

800m

600m

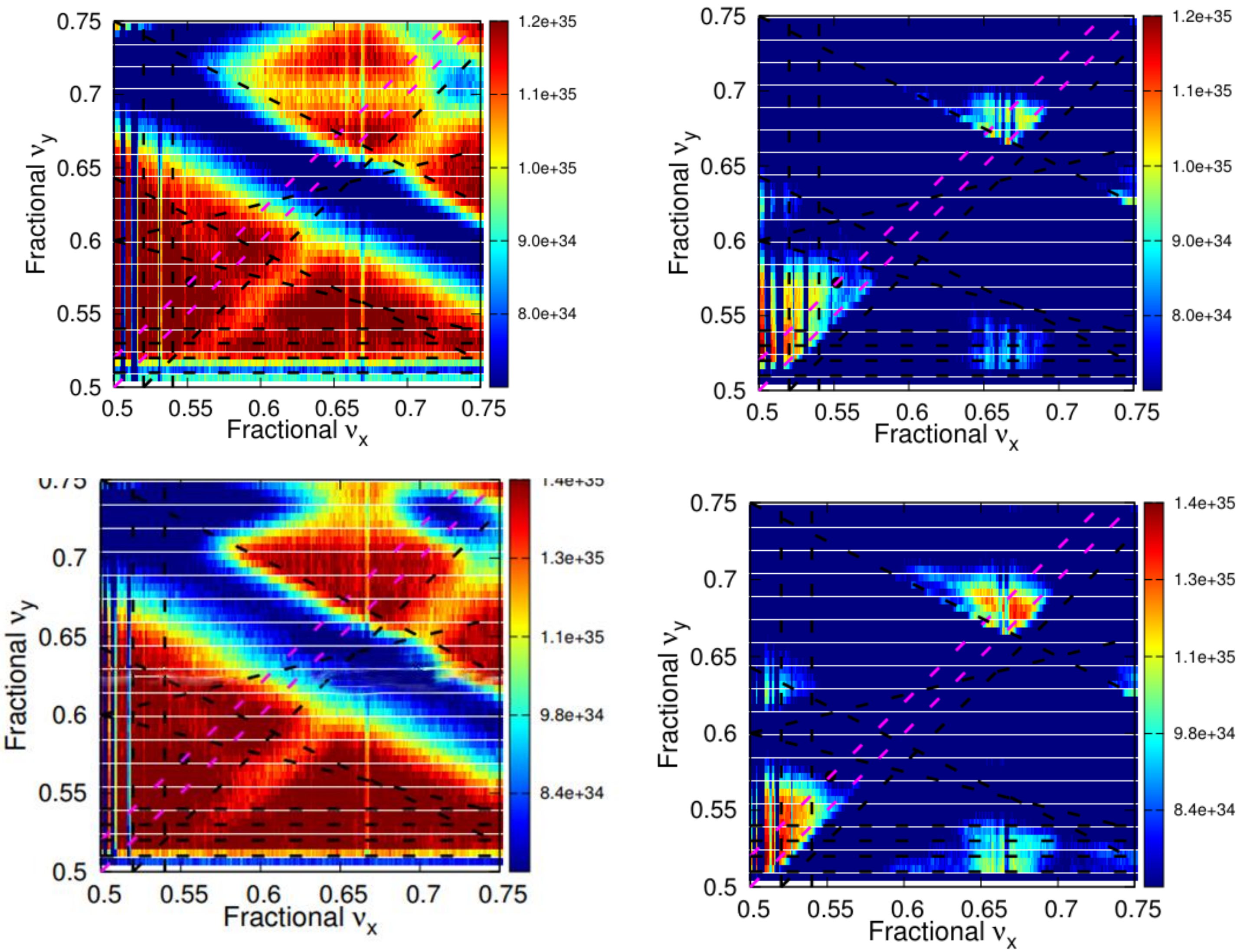

CW ON CW OFF

- CW has a more significant effect in increasing the area of the high-luminosity region for 800m.

Simulation result at the 800m working point：

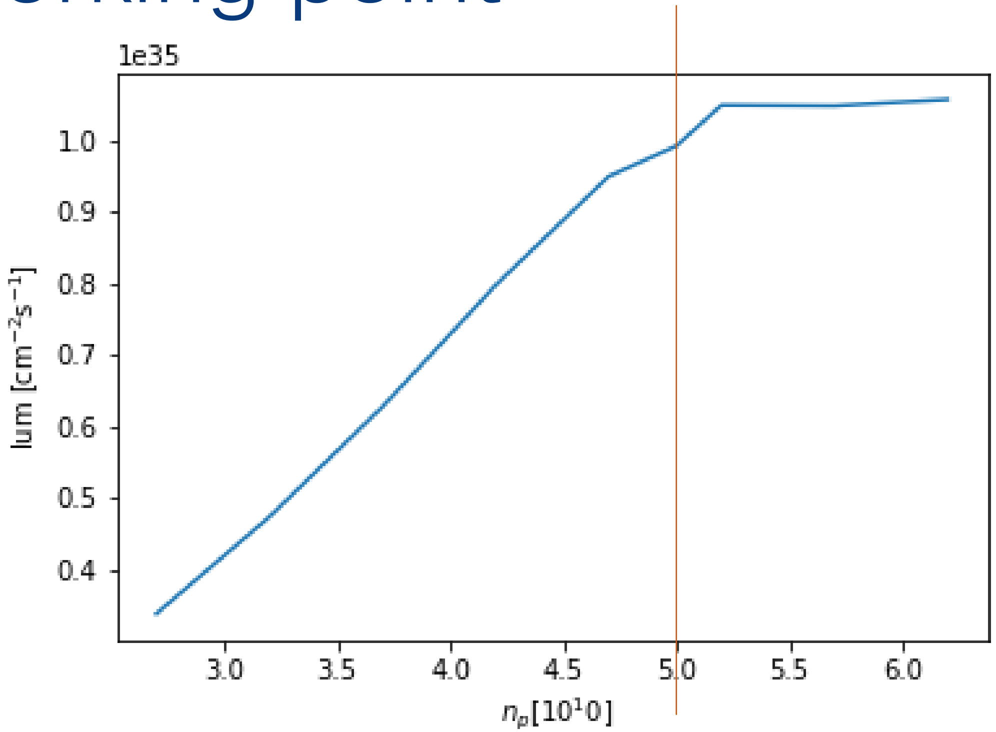

- The luminosity reaches the engineering design target.
- Slightly lower than the design luminosity.

STCF-CR-Para-V0

Parameters	Units	Value
Optimal beam energy, E	GeV	2
Circumference, C	m	847.76
Crossing angle, 2θ	mrad	60
L^*	m	0.9
Relative gamma		3913.9
Revolution period, T_0	μs	2.828
Revolution frequency, f_0	kHz	353.63
Horizontal emittance, ε_x	nm	7.532
Coupling, k		0.50%
Vertical emittance, ε_y	pm	37.66
Hor. beta function at IP, β_x	mm	40
Ver. beta function at IP, β_y	mm	0.6
Hor. beam size at IP, σ_x	μm	17.36
Ver. beam size at IP, σ_y	μm	0.150
Betatron tune, ν_x/ν_y		30.55/30.57
Momentum compaction factor, α_p	10^{-4}	12.29
Energy spread, σ_ε	10^{-4}	8.41
Beam current, I	A	2
Bunch filling ratio		50%
Number of bunches, n_b		707
Bunch spacing, ΔT_b	ns	4.0
Single-bunch current, I_b	mA	2.83
Particles per bunch, N_b	10^{10}	5.00
Total particles per beam	10^{13}	3.53
Single-bunch charge	nC	8.00
Energy loss per turn, U_0	keV	396.4
SR power per beam, P_{SR}	MW	0.7928
Hor. damping time, τ_x	ms	28.54
Ver. damping time, τ_y	ms	28.54
Long. damping time, τ_z	ms	14.27
RF frequency, f_{RF}	MHz	499.7
Harmonic number, h		1413
RF voltage, V_{RF}	MV	2
Synchronous phase, ϕ_s	deg	169
Synchrotron tune, ν_z		0.0165
Natural bunch length, σ_z	mm	8.47
RF bucket height, $(\Delta E/E)_{max}$	%	1.61
Piwinski angle, ϕ_{Piw}	rad	14.64
Hor. beam-beam parameter, ξ_x		0.0035
Ver. beam-beam parameter, ξ_y		0.090
Equivalent bunch length, σ_{z_e}	mm	0.58
Hour-glass factor, F_h		0.8663
Luminosity, L	$cm^{-2}s^{-1}$	1.13E+35

The results of the 800m luminosity scan with varying current intensity:

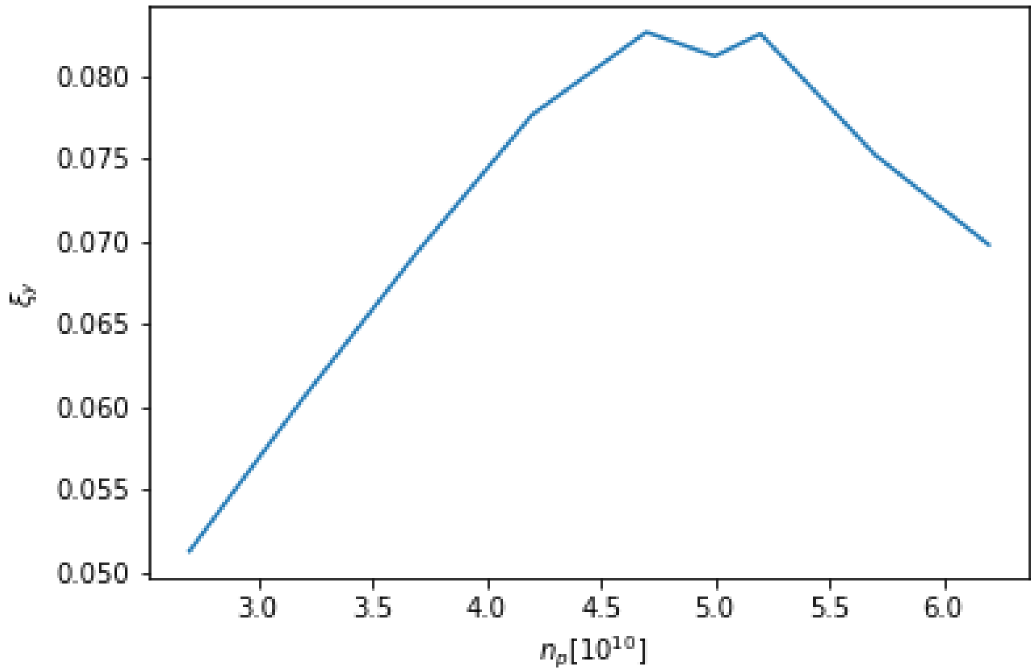

$$\xi_y = \frac{2r_e\beta_y}{N_{\pm}\gamma_{\pm}}\frac{L}{f_{\text{rep}}}$$

- The current threshold and beam-beam limit occur around np=4.5e10.
- Since 550 is not a stable working point, ξy does not remain constant but instead drops.

The results of FCCee:

K. Ohmi , FCCee optics meeting, Apr. 4, 2024

Bunch population dependence

- Luminosity

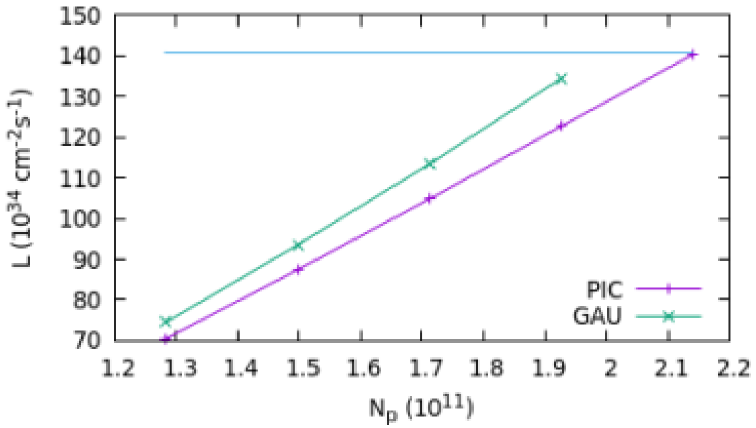

Specific lumi

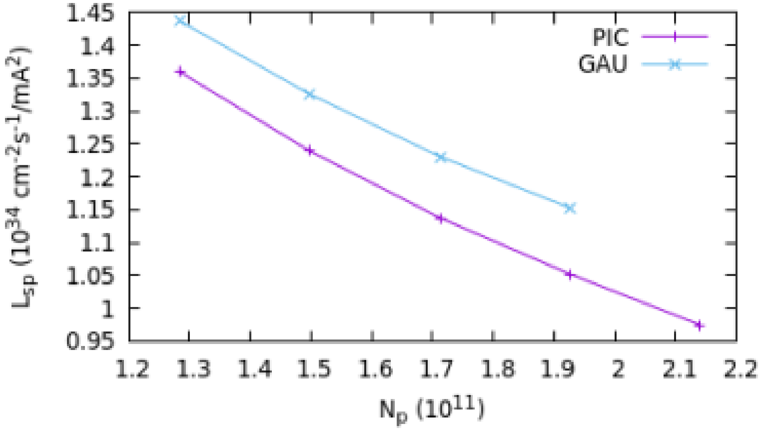

Normalized lumi

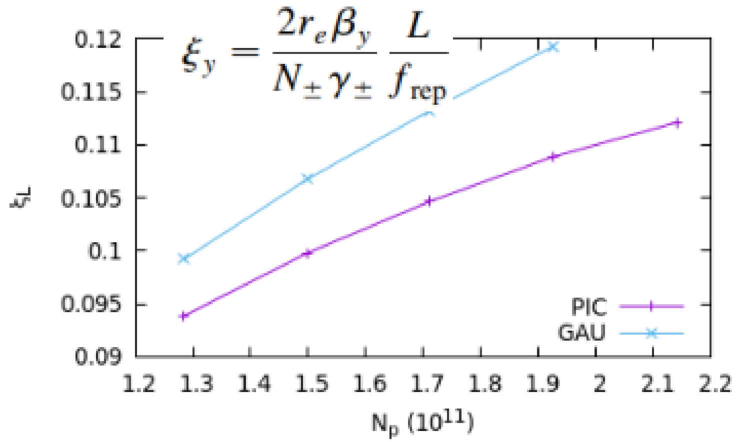

- The target luminosity is achieved.
- The beam loss affects the simulation result for SG in $N_p = 2.14 \times 10^{11}$.

The results of the 800m luminosity scan with varying current intensity:

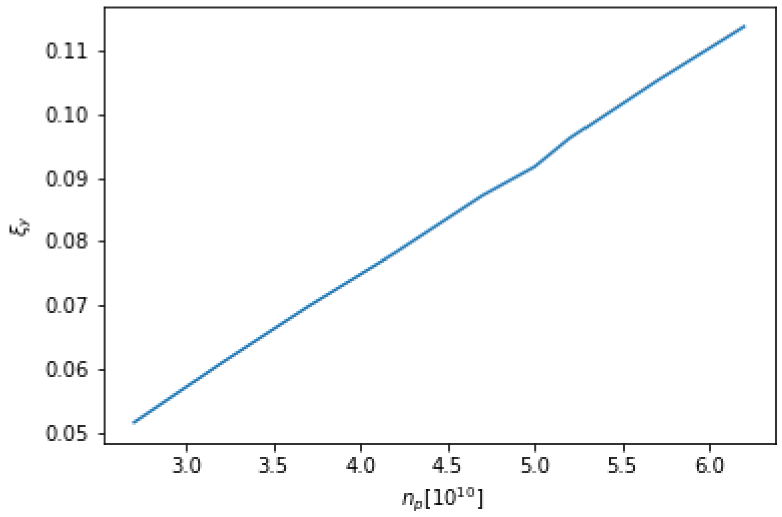

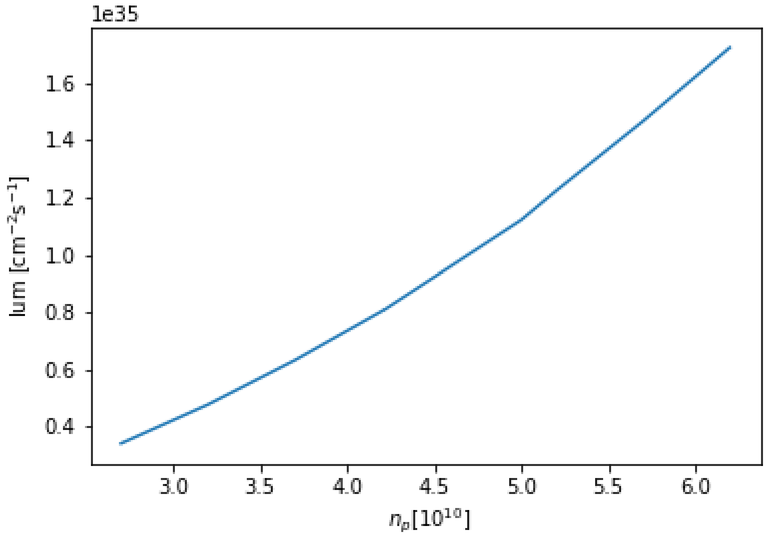

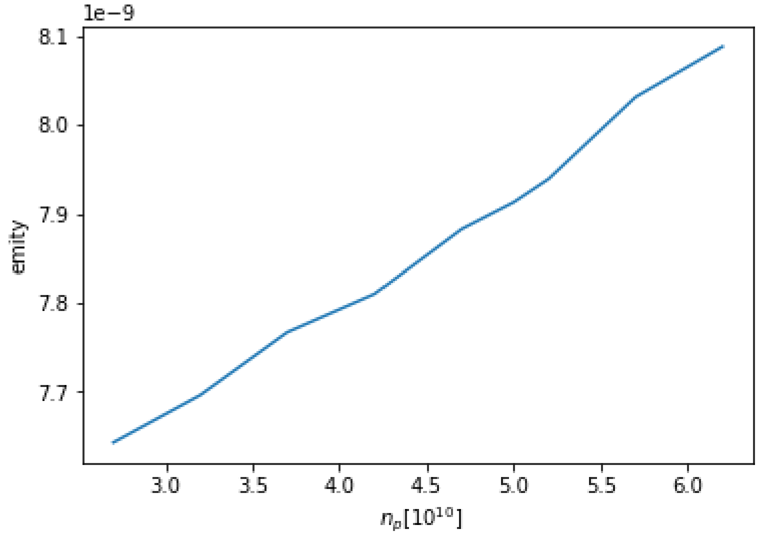

- After shifting the working point to 552, the ξy decay disappears.
- The beam-beam limit has not been reached when np≤6.2.

High-Luminosity Region Scan Near the 800m Working Point:

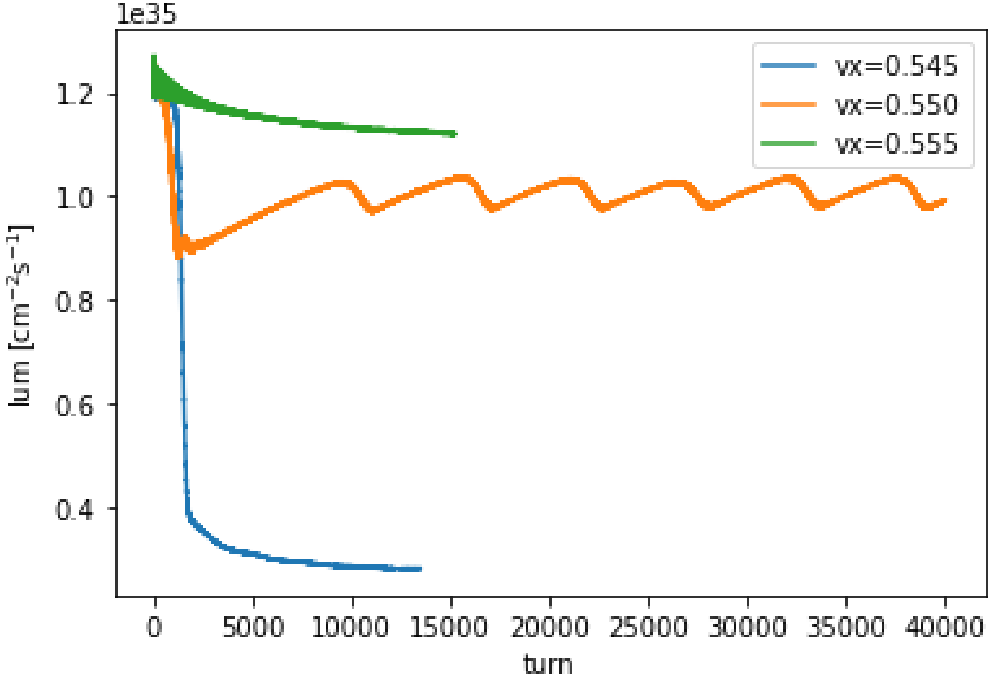

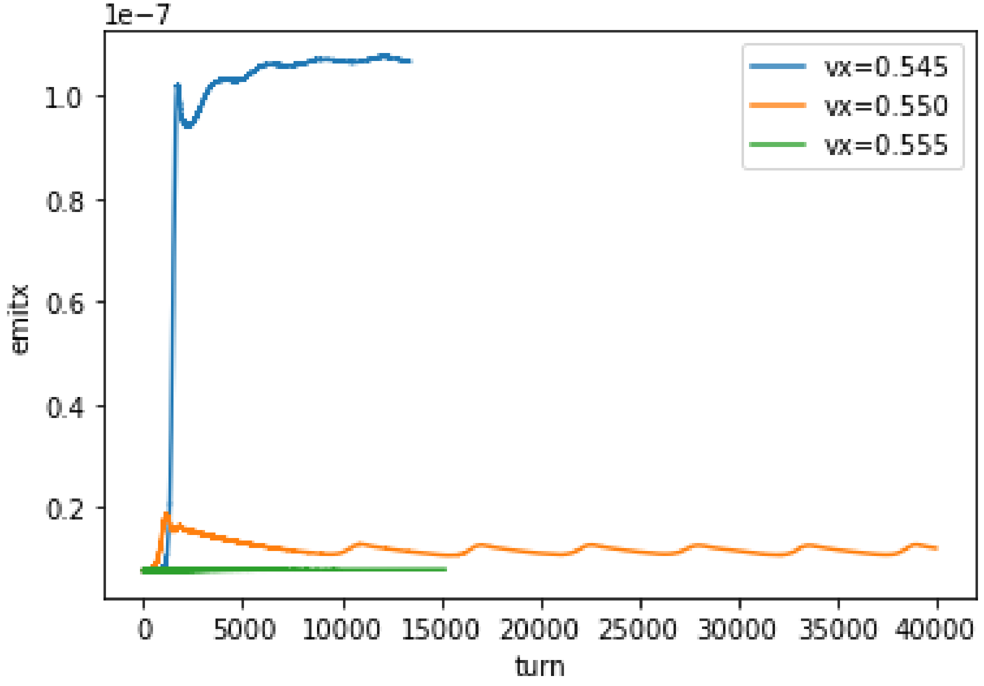

- There is unstable luminosity oscillation around 0.550.
- At 0.54x, in an unstable region, luminosity drops significantly.
- Luminosity at 0.55x remains mostly stable above the design luminosity of 1e35.

High-Luminosity Region Scan Near the 800m Working Point:

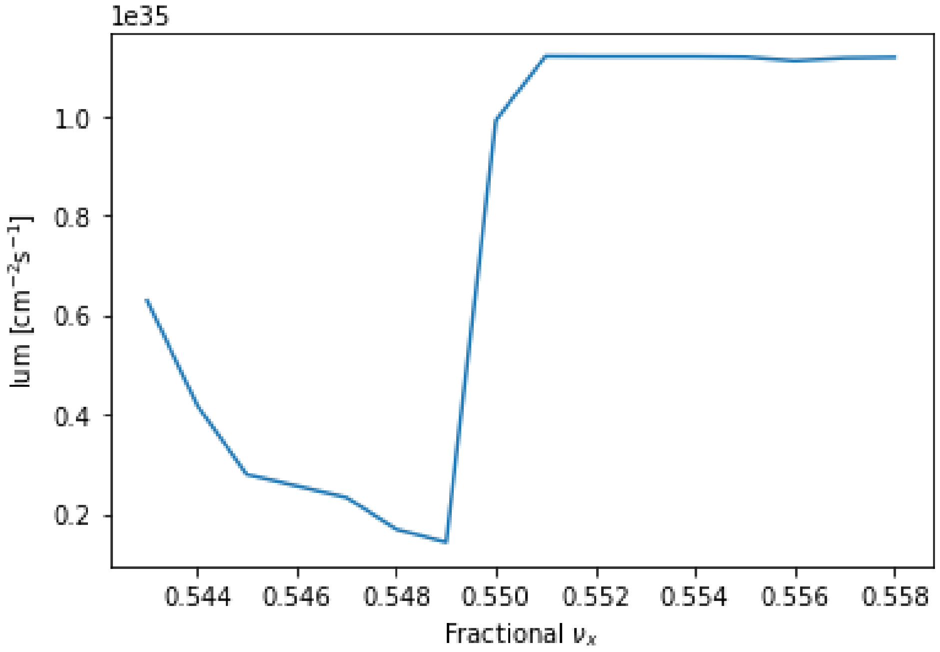

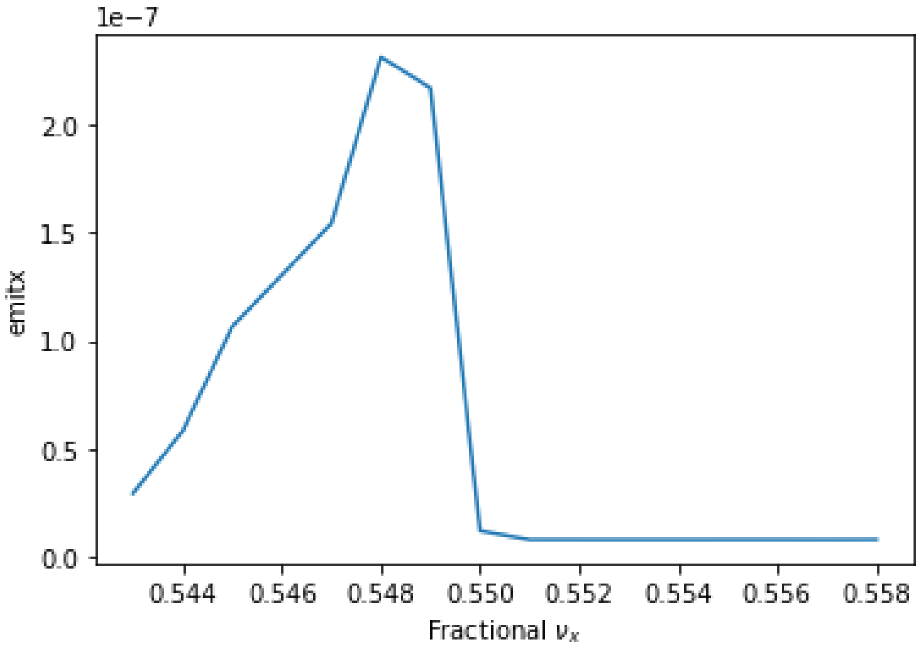

- The luminosity remains stable at around 1.12e35 in the range of 0.551–0.558.
- Luminosity near the 0.55 point is unstable.
- The current X-Z oscillation period is relatively large, nus=0.0165>5*ξ_x (0.0035).

Summary:

- The adjusted 800m structure is less susceptible to X-Z instability than the 600m structure and has a more stable luminosity region.
- The horizontal design working point for 800m requires a slight adjustment.

Ongoing Work:

- Conducting GPU-based beam-beam simulations with lattice for 800m.
- Simulating the coupling with impedance wakefields.
- Attempt to use methods such as Frequency Map Analysis (FMA) to further investigate the reasons behind the luminosity reduction caused by the beam-beam interaction when the lattice is introduced.

Acknowledgments

- Grateful thanks to Y. Zhang (IHEP), K. Ohmi (KEK), and D. Zhou (KEK) for their guidance and support, and to the teachers and colleagues for their help throughout this project.

Thank you!

Looking forward to your feedback and suggestions.

First edition lattice

parameters	values
Circumference /m	707.258
Beam energy/GeV	2*, 1-3.5
Crossing angle (2θ)/mrad	60
current/A	1.5
(β_x^*/β_y^*)/mm	64.1/0.638
ε$(\varepsilon_x/\varepsilon_y)$/nm·rad	2.85/0.0285
ν_x/ν_y	30.523 / 28.538
chromaticity(C_x/C_y)	-95.291/-346.239
Momentum compaction factor	1.237×10^{-3}
Energy spread	4.034×10^{-4}
Energy loss per turn/keV	78.4
(σ_x/σ_y)/μm	13.61/1.39
ξ_y	0.04-0.06 (estimate)
Hourglass factor	0.8 (estimate)
Luminosity/$\times10^{35}cm^{-2}s^{-1}$	0.63-0.95

- **Preliminary lattice design results (no nolinear)**

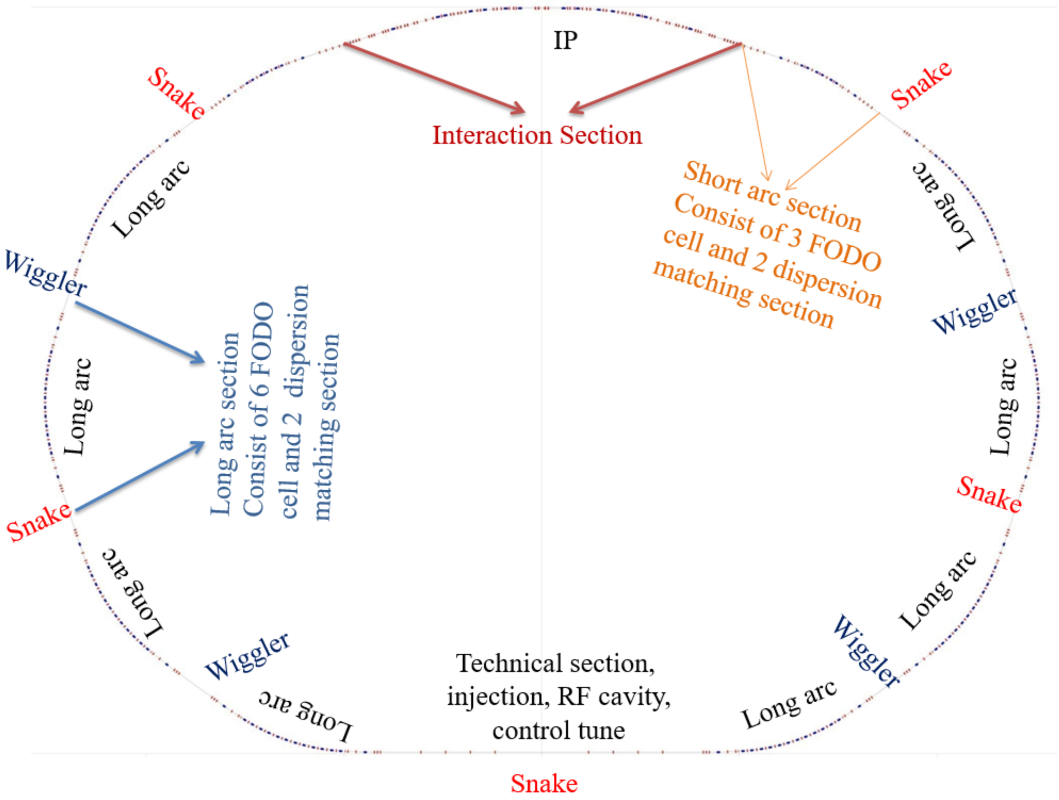

From Q. Luo "STCF-ACC Accelerator concept introduction and summary",2020.

Design of wiggler

❑ Add damping wiggler

- damping time :

52ms → 36ms

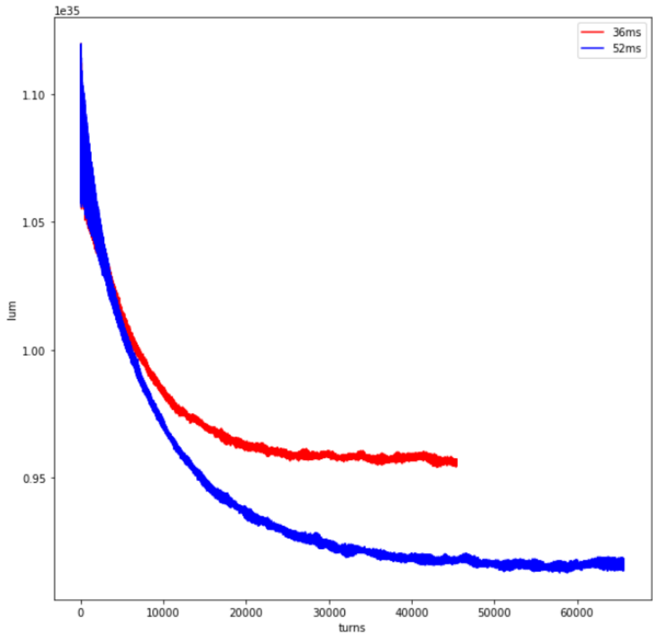

The luminosity of different damping time

(0.536,0.575,0.016)

	damping time/ms	lum at 1dt	lum at 2dt	lum at 3dt
12000	24.68	10.1225	10.025	10.015
16000	32.91	9.895	9.81	9.7975
17500	35.99	9.8225	9.7225	9.725
18180	37.39	9.79	9.685	9.6925
20000	41.13	9.7	9.62	9.5925
25000	51.42	9.4925	9.3725	/

design parameter of damping wiggler ：

Single DW length	1.8	m
Period	20	cm
Number of DW	4	
Field quality（x=1cm）	$<10^{-3}$	

Energy	1	1.5	2	2.5	GeV
Wiggler field B_w	5.1	3.7	2.3	0	T
Wiggler SR power per DW	59.3	70.2	48.2	0	kW
Damping intergral per DW	23.41	12.32	4.76	0	T^2m

Analysis of luminosity under different cross angles：

Both at （572， 552）

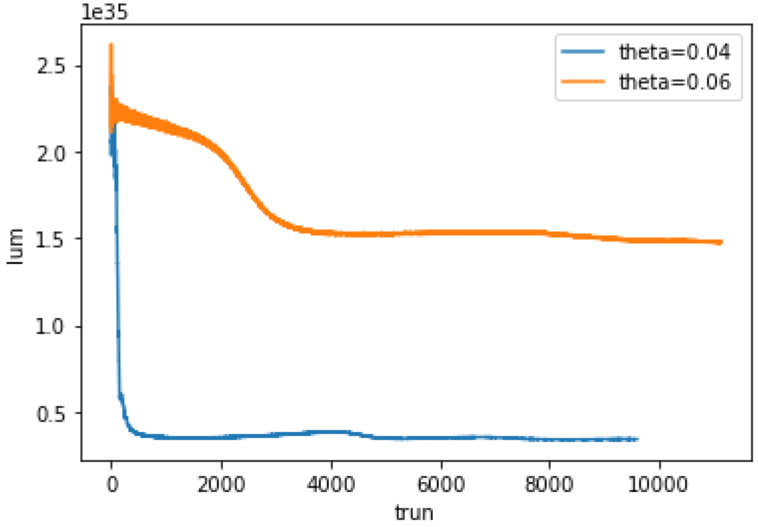

xangle (half) = 30.00 (mrad)

xangle (half) = 20.00 (mrad)

$$\mathcal{L} = H_D \frac{N^2 f_r n_b}{4\pi\sigma_x\sigma_y} \frac{1}{\sqrt{1+\left(\frac{\sigma_z}{\sigma_x}\tan\frac{\theta_c}{2}\right)^2}}$$

The longitudinal size is much larger than the transverse size.

$$\mathcal{L} = H_D \frac{N^2 f_r n_b}{4\pi\sigma_x\sigma_y} * \left(\frac{\sigma_x}{\sigma_z} / \tan\frac{\theta_c}{2}\right)$$

$$\mathcal{L}_{0.04}/\mathcal{L}_{0.06} = \theta_{0.06}/\theta_{0.04} = 1.5$$

Luminosity_0_0.04/ Luminosity_0_0.06
= 4.476E+32/ 3.137E +32
≈1.427

The y-direction increases by about eight times

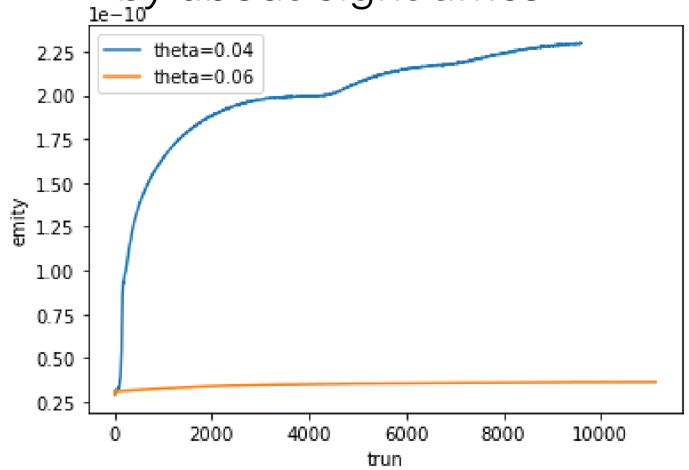

the X-direction increases by about twice

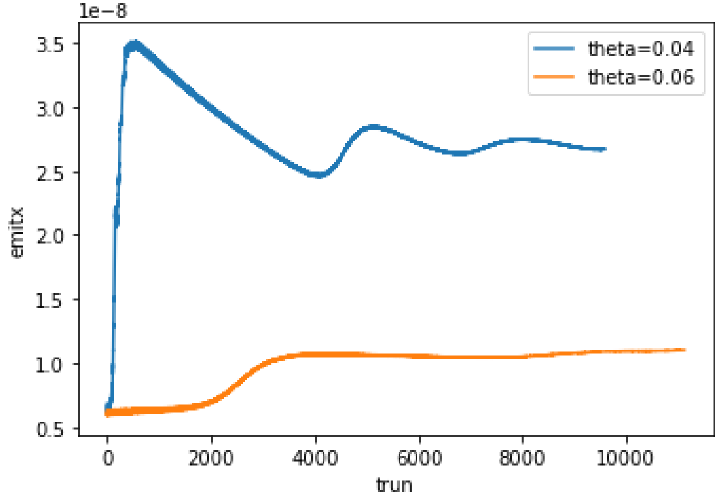

- The initial luminosity satisfies the formula relation, but the luminosity decreases due to blow-up in the vertical direction.

WS result vs SS result

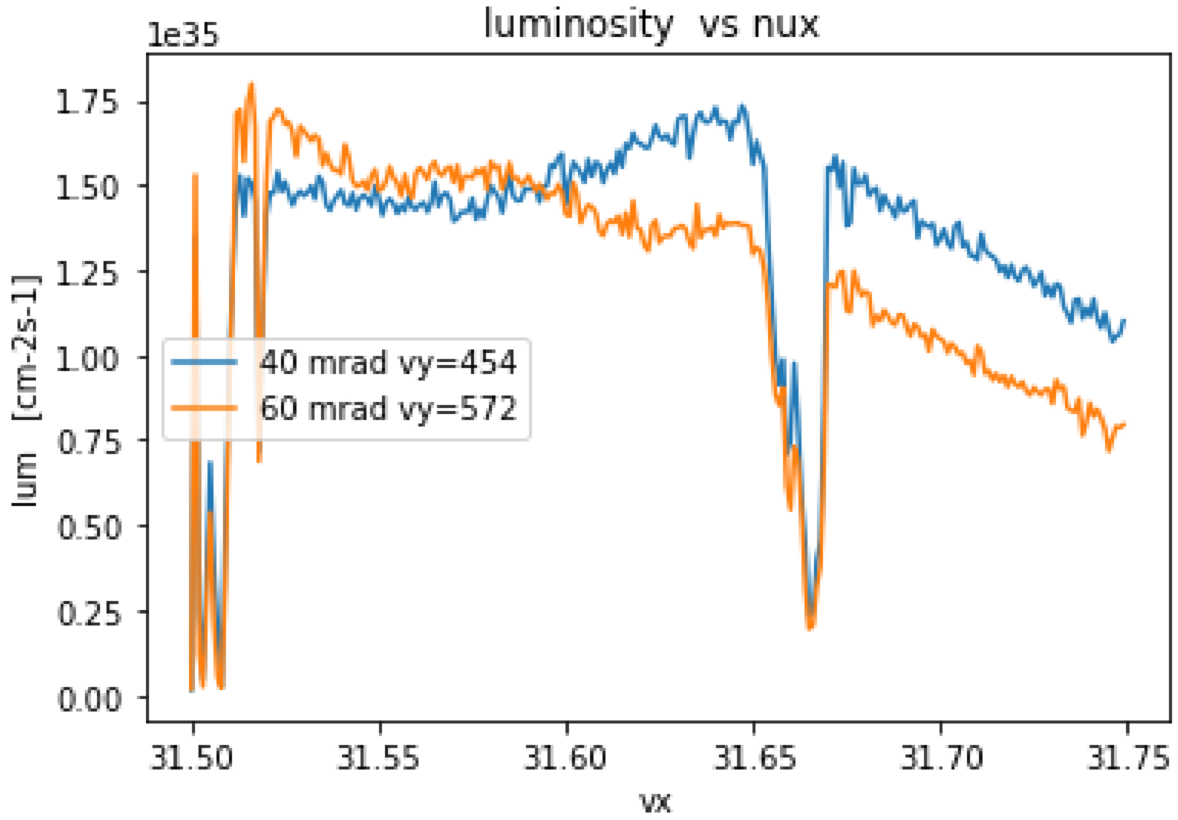

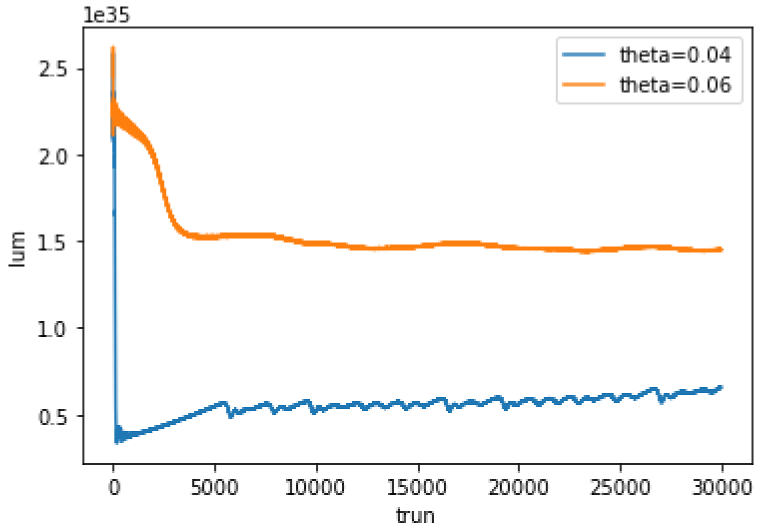

xangle (half) = 30.00 (mrad) (572, 552)

xangle (half) = 20.00 (mrad) (545, 550)

- Unstable for 0.04 when SS simulation.

XZ Instability at Different Crossing Angles:

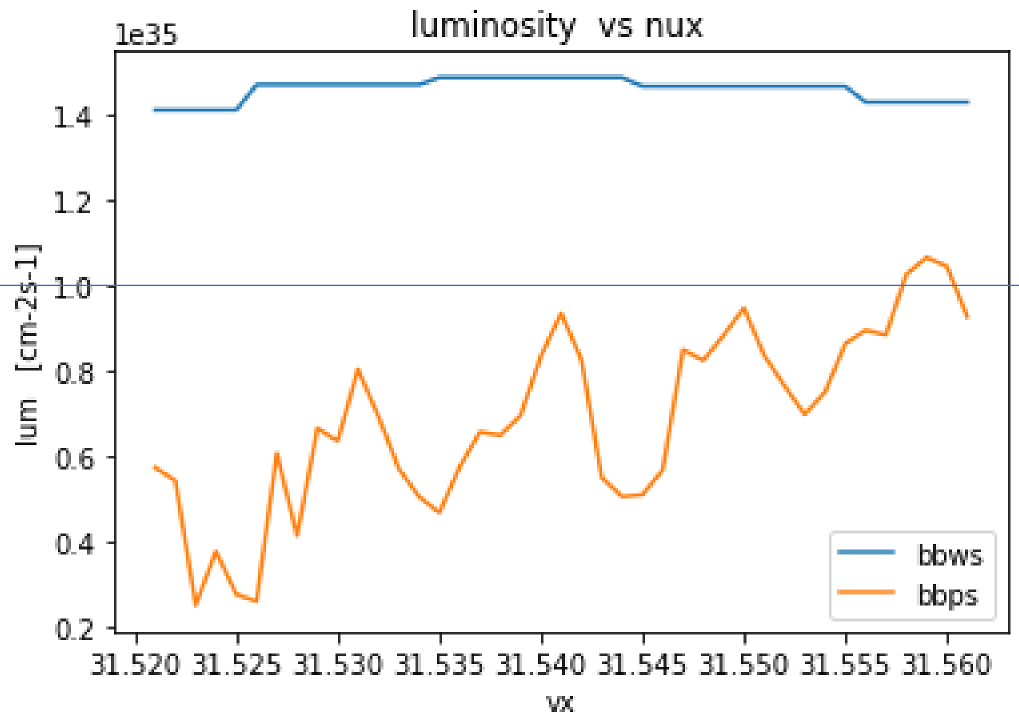

2θ =0.04 nvy = .545

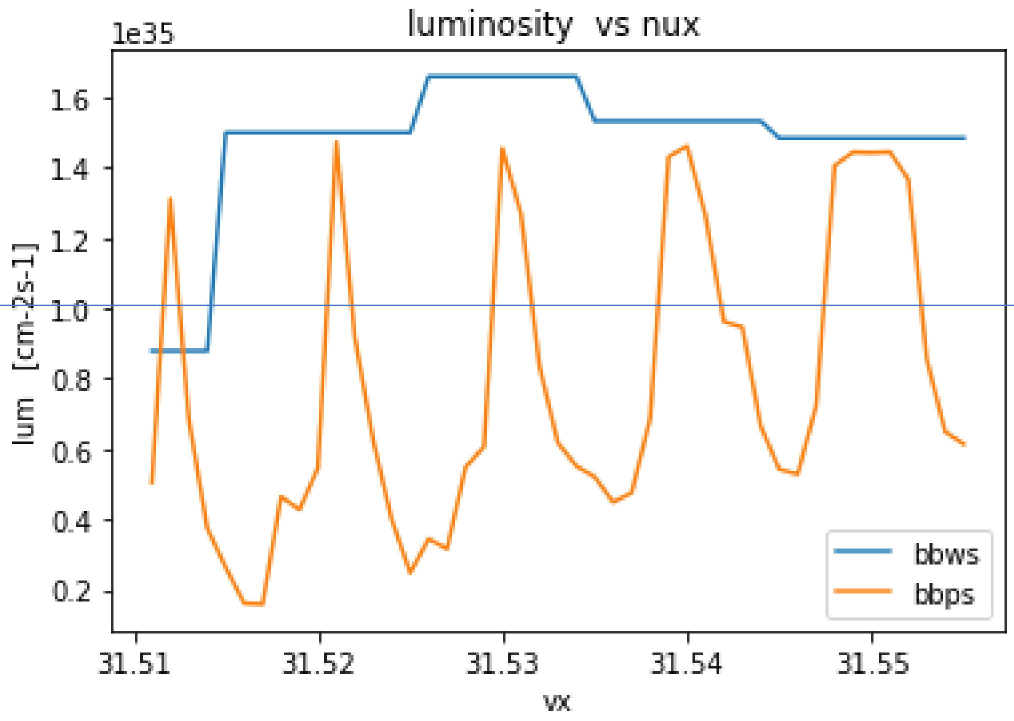

2θ =0.06 nvy = .572

The results of the 800m luminosity scan with varying current intensity：

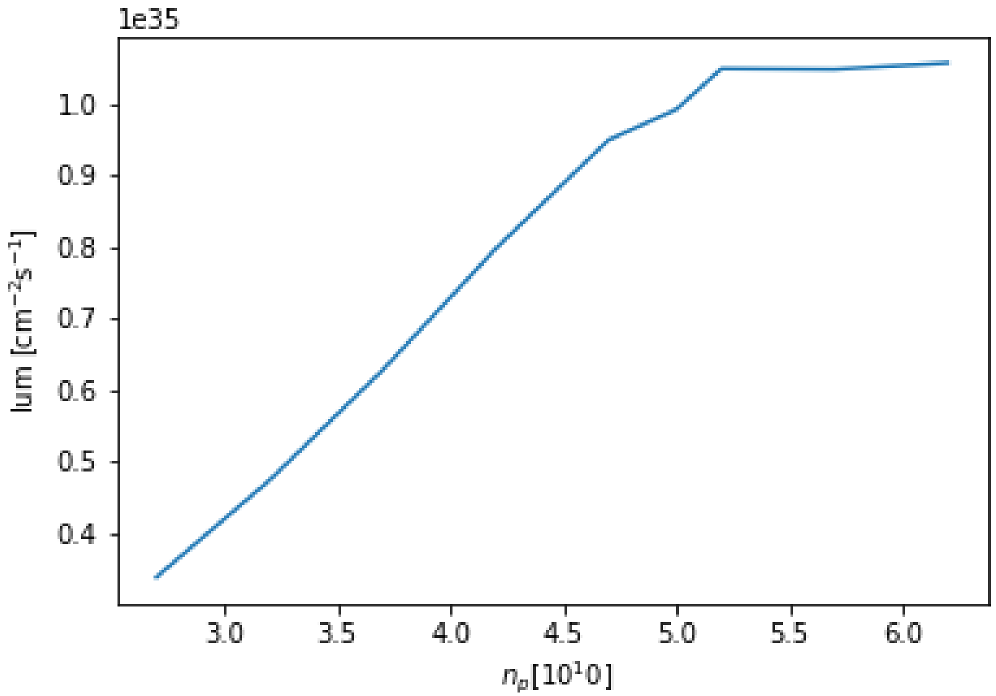

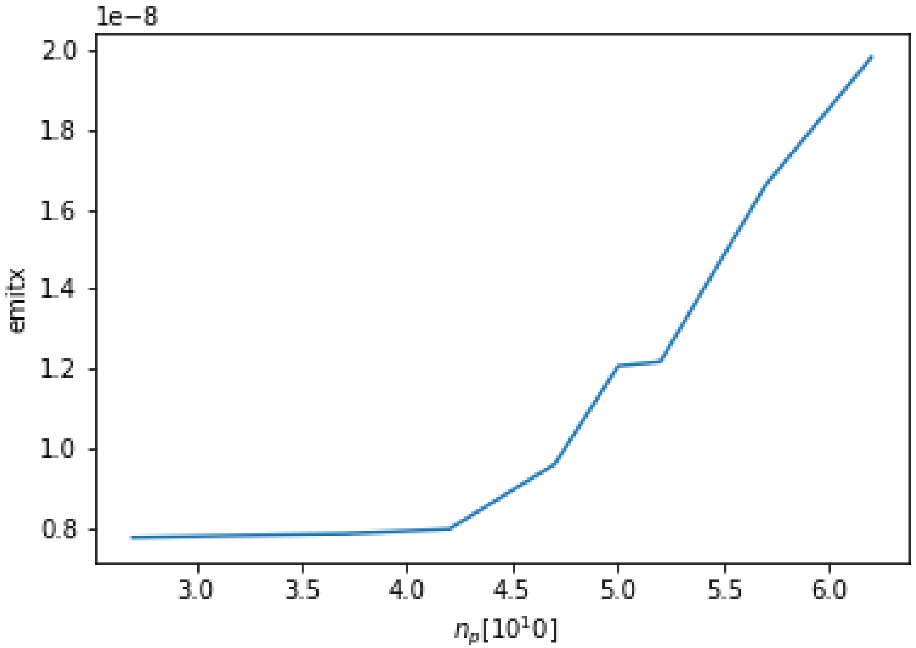

- After np>5.2, the luminosity no longer increases with the number of particles.
- The increase in emittance occurs earlier.

The results of the 800m luminosity scan with varying current intensity:

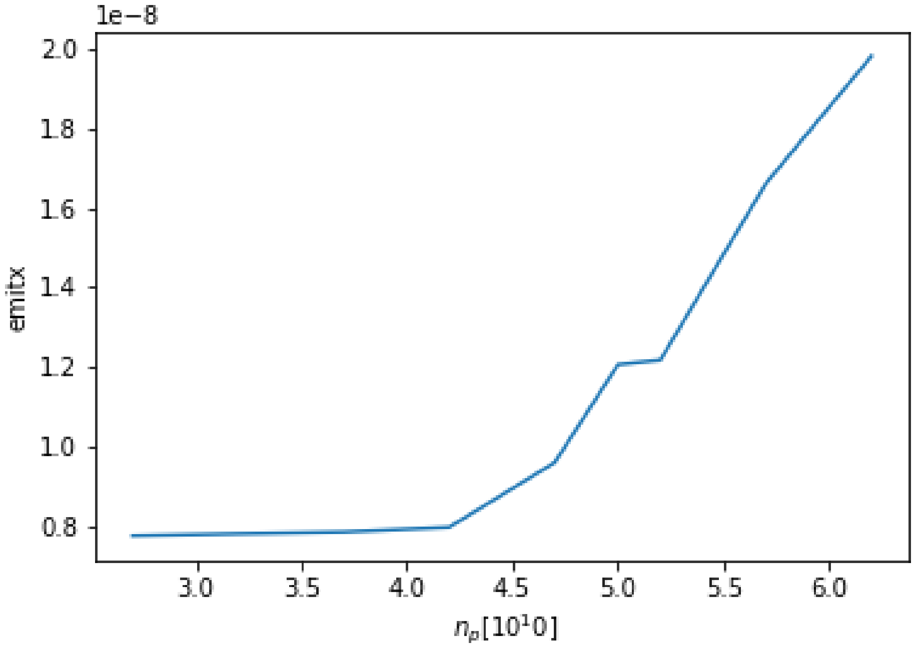

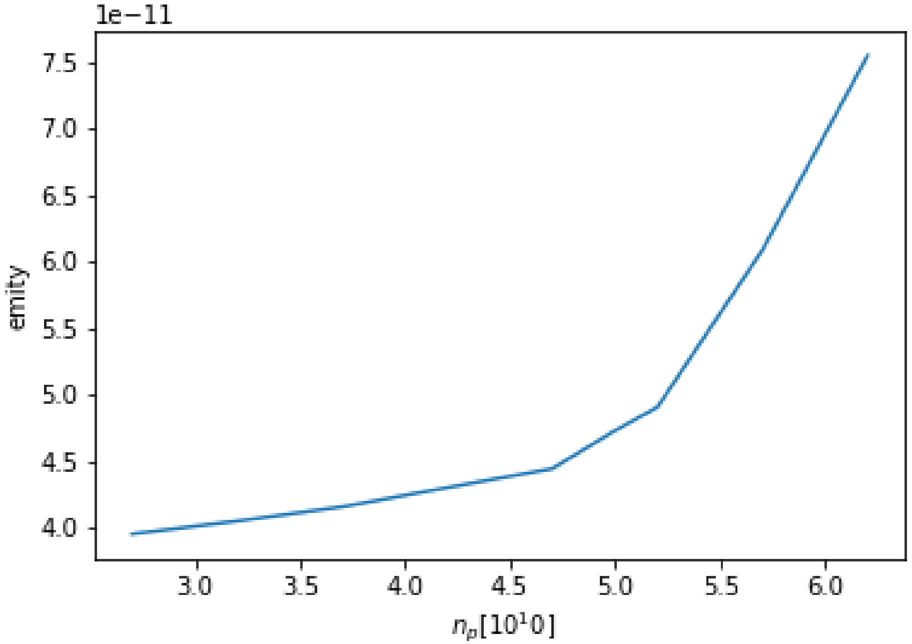

- The horizontal emittance growth precedes the vertical emittance growth.
- The horizontal emittance begins its first rapid increase at np>4.2.
- The rapid increase in vertical emittance starts at np>4.7, coinciding with the second rapid increase in horizontal emittance.

The results of the 800m luminosity scan with varying current intensity:

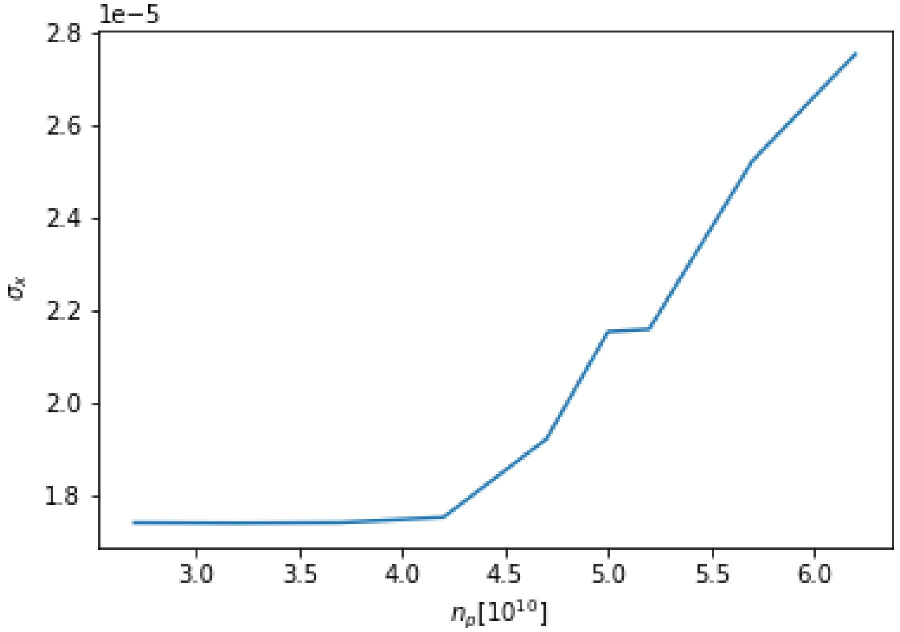

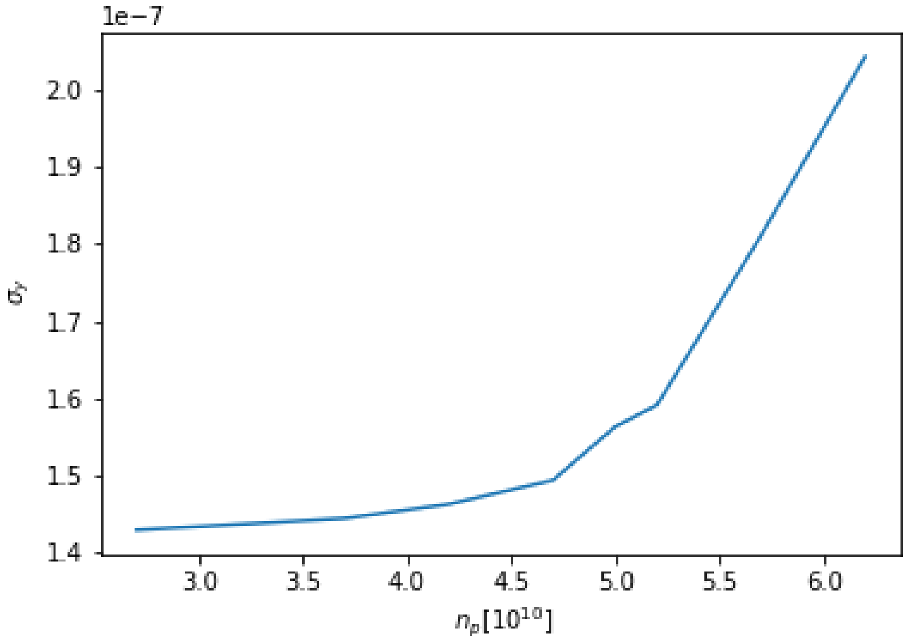

- The growth is mainly related to σx and has little to do with $\sigma x'$.
- The second rapid vertical growth and the third rapid horizontal growth occur together at $np > 5.2$.

WS scan

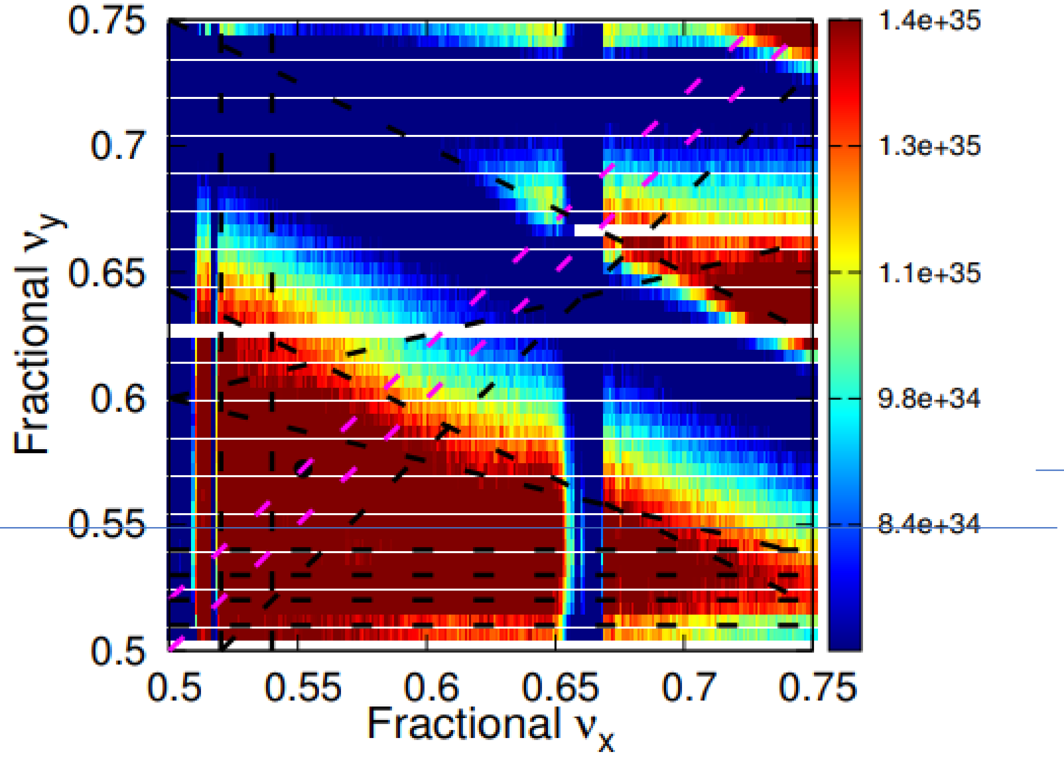

2θ =0.04

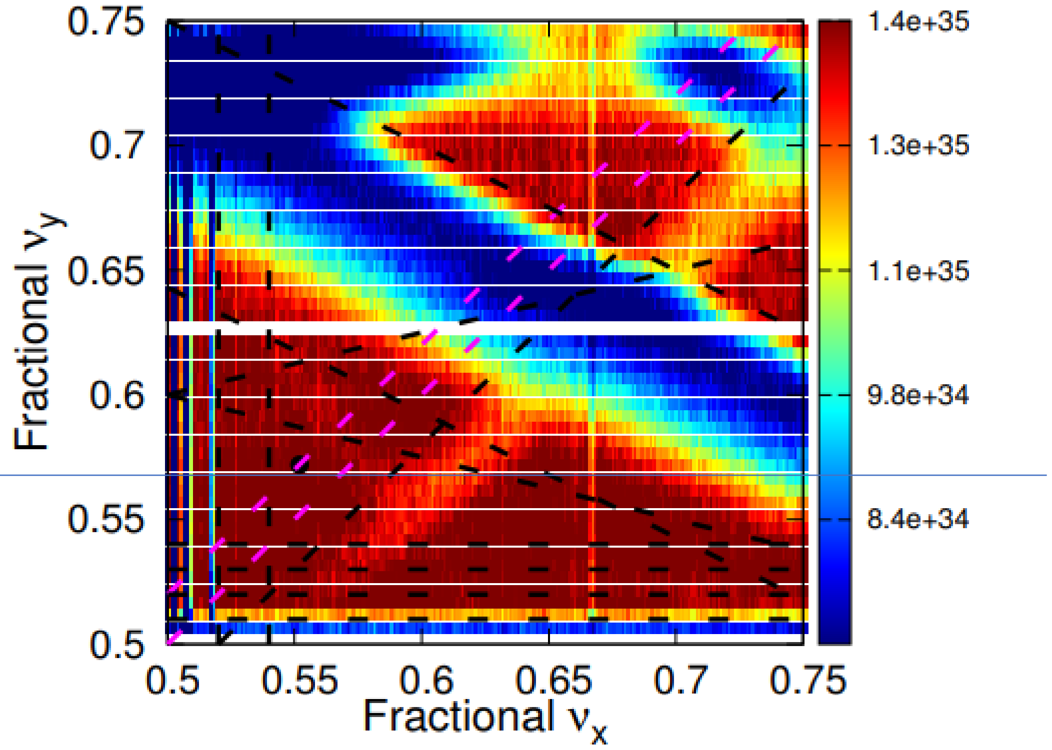

2θ=0.06(design)

- The luminosity does not significantly increase when the crossing angle is decreased.

Longitudinal dynamics design considerations

➢Coherent X-Z instability

- A newly discovered coherent beam-beam interaction under a large Piwinski angle using strong-strong beam-beam simulations
  - → primarily leads to an increase in the horizontal emittance ε_x
  - → Considering the coupling between horizontal and vertical emittances, it eventually results in an increase in the vertical emittance ε_y and a collapse of the luminosity
- This instability cannot be suppressed through beam feedback systems, but can only be avoided through appropriate parameter optimization
  - →Typically, a stringent requirement of $\xi_x \ll \nu_z$ is imposed to have wide region for the selection of working point without beam blow-up
  - →In the case of STCF, $\nu_z/\xi_x \geq 3$ is expected.

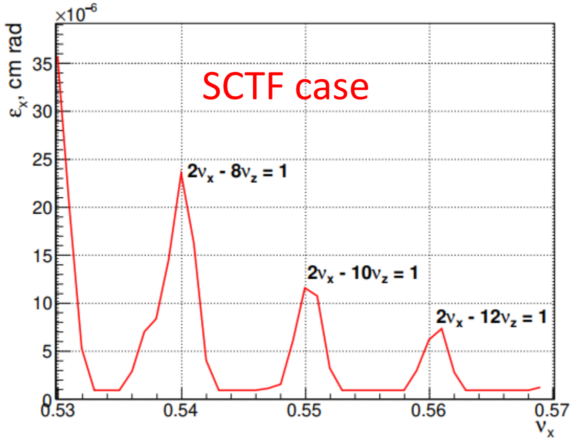

Figure 1.28. Growth of ε_x due to coherent X-Z instability, as a function of ν_x.

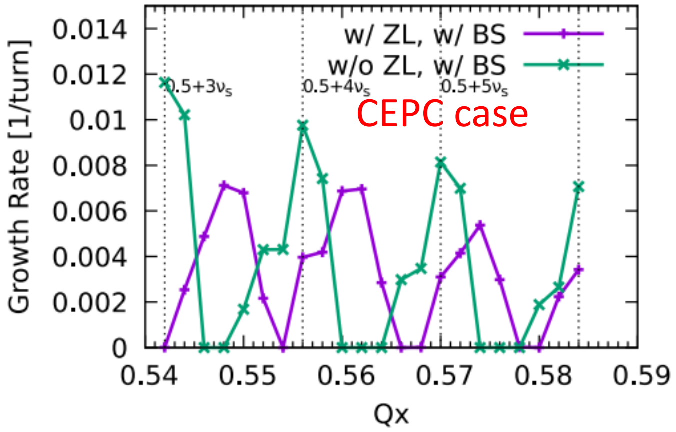

Longitudinal dynamics design considerations

➢Lattice Design and Damping Wigglers

- **Lattice design** is crucial for achieving high luminosity by achieving the required optical parameters at IP and by optimizing nonlinear dynamics aperture
- Additionally, it defines the momentum compaction factor α_p and natural energy spread σ_δ in the electron storage ring through synchrotron radiation integrals.

  ✓ These parameters (α_p and σ_δ) are of importance in the longitudinal dynamics

$$\alpha_p = \frac{I_1}{C_0} \qquad \sigma_\delta^2 = C_q \gamma^2 \frac{I_3}{j_z I_2}$$

- **Damping wigglers** are essential for STCF to control the damping time (30 ms) and to maintain beam emittance almost constant (~5 nm) throughout the entire energy range 1—3.5 GeV.

  ✓ This inevitably increases the synchrotron radiation energy loss per turn

  → raising the demand for RF power

$$\tau_x = \frac{2E}{\mathcal{J}_x U_0} T_0 \qquad U_0 = \frac{C_\gamma}{2\pi} E_0^4 I_2$$

  ✓ This also increases the natural energy spread

  → resulting in a proportional growth in bunch length

$$\sigma_\delta^2 = C_q \gamma^2 \frac{I_3}{j_z I_2}$$

- The lattice including damping wigglers has been designed for STCF at 2 GeV

Longitudinal dynamics design considerations

➢Non-impedance-induced collective effects

- **Intrabeam scattering (IBS):** multiple small-angle Coulomb scattering processes
  - $\rightarrow$ not immediately cause particle loss in the bunch
  - $\rightarrow$ but increase the equilibrium energy spread, bunch length, and transverse emittances
- **Touschek effect:** single large-angle scattering processes
  - $\rightarrow$ A large momentum deviation (beyond RF momentum acceptance or physical aperture)
  - $\rightarrow$ thus limit the lifetime of the stored beam (i.e., the Touschek lifetime)
- These two effects are directly related to the 6D phase-space size and thus associated with longitudinal parameters such as the bunch length
- elegant and SAD codes can be used to calculate IBS and the Touschek lifetime

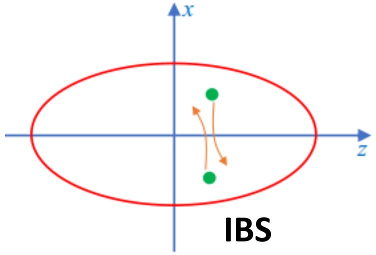

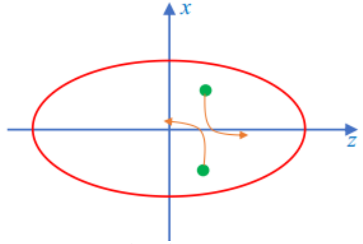

➢Impedance-induced single-bunch collective effects

- bunch lengthening due to potential well distortion (PWD) $\left(\frac{\sigma_z}{\sigma_{z0}}\right)^3 - \frac{\sigma_z}{\sigma_{z0}} = \frac{I_b \alpha_p}{4\sqrt{\pi}\nu_z^2 E/e}\left(\frac{R}{\sigma_{z0}}\right)^3 \mathrm{Im}\left(\frac{Z_\parallel}{n}\right)_{\mathrm{eff}}$
- longitudinal microwave instability (LMWI) $I_b^{\mathrm{mwi}} = \frac{\sigma_z}{R}\frac{\sqrt{2\pi}\alpha_p E/e}{\left|Z_\parallel/n\right|_{\mathrm{eff}}}\sigma_\delta^2$
- transverse mode coupling instability (TMCI) $I_b^{\mathrm{tmci}} = \frac{\sigma_z}{R}\frac{4\sqrt{\pi}\nu_z E/e}{\langle\beta\rangle \cdot \mathrm{Im}Z_\perp^{\mathrm{eff}}}$